Shallow-Water Wave Calculations

D. O. Hodgins, P.H. LeBlond, and D.A. Huntley*

Marine Environmental Data Services Branch
Department of Fisheries and Oceans
Ottawa, Ontario K1A 0E6

June 1985

Canadian Contractor Report of Hydrography and Ocean Sciences No. 10

*Seaconsult Marine Research Ltd., Vancouver

3-5996/

Canadian Contractor Report of Hydrography and Ocean Sciences

Contractor reports are unedited final reports from scientific and technical projects contracted by the Ocean Science and Surveys (OSS) sector of the Department of Fisheries and Oceans.

The contents of the reports are the responsibility of the contractor and do not necessarily reflect the official policies of the Department of Fisheries and Oceans.

If warranted, contractor reports may be rewritten for other publications of the Department, or for publication outside the government.

Contractor reports are abstracted in *Aquatic Sciences and Fisheries Abstracts* and indexed in the Department's annual index to scientific and technical publications.

Contractor reports are produced regionally but are numbered nationally. Requests for individual reports will be filled by the issuing establishment listed on the front cover and title page. Out of stock reports will be supplied for a fee by commercial agents.

Regional and headquarters establishments of Ocean Science and Surveys ceased publication of their various report series as of December 1981. A complete listing of these publications is published in the *Canadian Journal of Fisheries and Aquatic Sciences*, Volume 39: Index to Publications 1982. The current series, which begins with report number 1, was initiated in January 1982.

Rapport canadien des entrepreneurs sur l'hydrographie et les sciences océaniques

Cette série se compose des rapports finals non révisés préparés dans le cadre des projets scientifiques et techniques réalisés par des entrepreneurs travaillant pour le service des Sciences et levés océaniques (SLO) du ministère des Pêches et des Océans.

Le contenu des rapports traduit les opinions de l'entrepreneur et ne reflète pas nécessairement la politique officielle du ministère des Pêches et des Océans.

Le cas échéant, certains rapports peuvent être rédigés à nouveau de façon à être publiés dans une autre série du Ministère, ou à l'extérieur du gouvernement.

Les rapports des entrepreneurs sont résumés dans la publication *Résumés des sciences halieutiques et aquatiques* et ils sont classés dans l'index annuel des publications scientifiques et techniques du Ministère.

Les rapports des entrepreneurs sont produits à l'échelon régional, mais numérotés à l'échelon national. Les demandes de rapports seront satisfaites par l'établissement auteur dont le nom figure sur la couverture et la page du titre. Les rapports épuisés seront fournis contre rétribution par des agents commerciaux.

Les établissements des Sciences et levés océaniques dans les régions et à l'administration centrale ont cessé de publier leurs diverses séries de rapports en décembre 1981. Une liste complète de ces publications figure dans le volume 39, Index des publications 1982 du *Journal canadien des sciences halieutiques et aquatiques*. La série actuelle a commencé avec la publication du rapport numéro 1 en janvier 1982.

Canadian Contractor Report of
Hydrography and Ocean Sciences 10

June 1985

SHALLOW-WATER WAVE CALCULATIONS

by

D.O. Hodgins, P.H. LeBlond and D.A. Huntley
Seaconsult Marine Research Ltd.
Suite 405 - 1200 West 73rd Avenue
Vancouver, British Columbia
Canada V6P 6G5

Marine Environmental Data Services Branch
Department of Fisheries and Oceans
Ottawa, Ontario
K1A 0E6

This report was prepared by:

Seaconsult Marine Research Ltd., Vancouver, British Columbia, under DSS Contract OSS82-00174.

Scientific Authority - J.R. Wilson, MEDS.

Correct citation for this publication:

Hodgins, D.O., P.H. LeBlond, and D.A. Huntley. 1985. Shallow-water wave calculations. Can. Contract. Rep. Hydrogr. Ocean Sci. 10:75 p.

©Minister of Supply and Services Canada 1985

Cat. No. Fs 97-17/10E ISSN 0711-6748

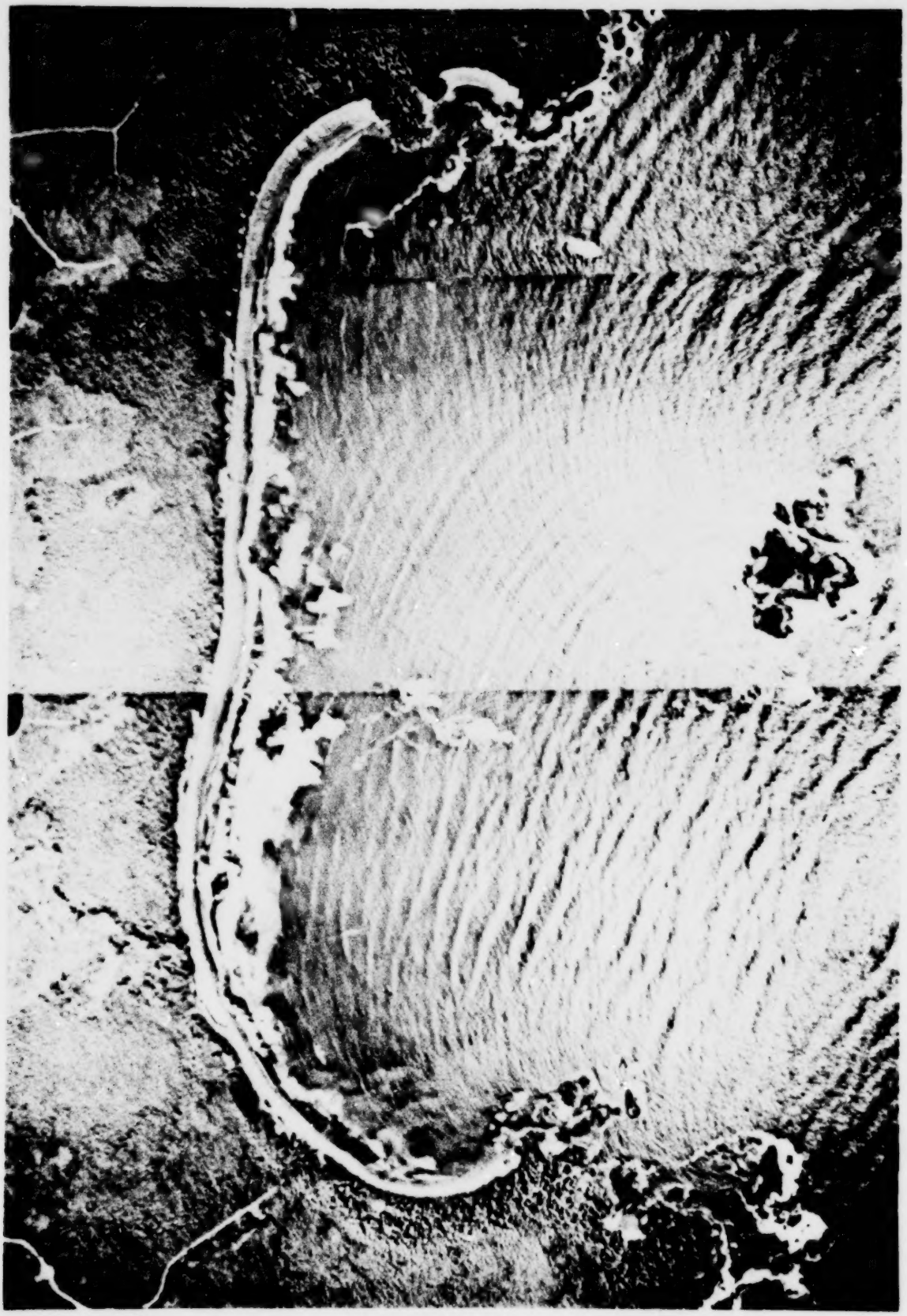

Frontispiece Wave refraction and diffraction patterns in Wreck Bay, Vancouver Island. (From Brenner, 1970).

Shallow – Water
Wave Calculations

ABSTRACT

Hodgins, D.O., P.H. LeBlond, and D.A. Huntley. 1985. Shallow-water wave calculations. Can. Contract. Rep. Hydrogr. Ocean Sci. 10:75 p.

This report discusses the numerical calculation of wave transformations. The discussion has particular application to the problem of relating shallow water wave conditions to offshore waves provided by a deep water wind-wave hindcast model.

Recent research into wave transformations is reviewed and, in particular, the application of methods where the wave conditions are described by directional spectra.

This is followed by a review of the current status of numerical modelling and the practical considerations of the application of existing models to Canadian waters.

RÉSUMÉ

Hodgins, D.O., P.H. LeBlond, and D.A. Huntley. 1985. Shallow-water wave calculations. Can. Contract. Rep. Hydrogr. Ocean Sci. 10:75 p.

Le présent rapport traite du calcul numérique de la transformation des vagues. La discussion s'applique en particulier au problème consistant à lier les conditions des vagues en eaux peu profondes aux vagues du large qui sont fournis par un modèle de prévisions à posteriori des vagues de vent.

On examine les recherches récentes sur la transformation des vagues et en particulier l'application de méthodes où les conditions des vagues sont décrites par des spectres directionnels.

Cette discussion est suivie de l'examen de la situation actuelle concernant la modélisation numérique et des observations d'ordre pratique sur l'application des modèles existants aux eaux canadiennes.

TABLE OF CONTENTS

	Page
Abstract/Résumé	vii
List of Tables	x
List of Figures	xi
1. Introduction	1
2. Shoaling and Refraction	
2.1 Plane Waves	3
2.2 Refraction by Current	4
2.3 Refraction of Wave Spectra	5
2.4 Computational Methods	7
2.5 Nonlinear Wave Refraction	9
3. Dissipative Processes	
3.1 Boundary Layer Friction	13
3.2 Percolation	18
3.3 Bottom Motion	21
3.4 Back Scattering	23
3.5 Finite Amplitude Effects	23
3.6 Wave Breaking	30
3.7 Wave Generation	33
4. Status of Shallow Water Wave Models	
4.1 Factors Affecting the Accuracy of Ray Tracing	
4.1.1 Parameterization of Depth	35
4.1.2 Treatment of Caustics	37
4.1.3 Comparisons with Observations	41
4.2 Applications of Shallow Water Wave Models	
4.2.1 Spectral Models	41
4.2.2 A Simplified Wave Height Model	48
4.2.3 A Non-Spectral Model	52
5. Toward Practical Modelling Systems	
5.1 Consideration of Scales, Resolution and the Consequences	59
5.2 A Recommended Strategy	63
6. References	66

LIST OF TABLES

Table	Title	Page
3.1	Exponential damping coefficients D [wave amplitude proportional to exp(-Dx)] for waves of period T=15 s, height H, length L and group velocity c_G in various water depths h and for three types of sediments.	24
5.1	Scales and resolution requirements for a wave modelling system.	61

LIST OF FIGURES

Figure	Title	Page
2.1	Comparison of observed and computed breaker wave heights, Broken Bay, Australia.	11
3.1	Friction factor diagram showing the variation in C_f with Reynolds number and bottom roughness for a rigid bottom (after Kamphuis, 1978).	15
3.2	Ripple steepness ζ/λ_s, against dimensionless bottom stress θ_s.	17
3.3a	Comparison between dissipation mechanisms.	19
3.3b	Relative significance of wave transformation mechanisms as a function of $k_p h$, where k_p is the wave number at the peak of the deep water spectrum and h the depth.	20
3.4	Comparison of Yamamoto's (1982) damping theory with laboratory data.	22
3.5	Photograph of regular waves refracting near a coastline, with possible wave splitting near the left-hand point (additional crests appearing between the regular wave crests next to the coast) (Photo courtesy of Dr. George L. Pickard).	26
3.6	a) The generation of harmonics in shoaling waves; b) comparison between predicted and observed spectra.	28
3.7	Comparison of power spectra between measured data ("DATA"), the Boussinesq model ("BOUSS"), another non-linear model used by Freilich ("CONSIS") and linear theory ("LINEAR").	29
3.8	Wave spectrum change due to shoaling and breaking.	32
4.1	Example of a conventional refraction diagram after Abernethy and Gilbert (1975).	37
4.2	Segment of conventional refraction diagram using closely spaced rays ($0.2\lambda_o$).	38
4.3	Computed and observed spectra using parallel bottom topography and irregular bottom topography from Collins (1972).	43

Figure	Title	Page
4.4	Spectra of six records during March 10, 1976, storm; 95% confidence limits are shown aside spectrum of record number 1.	45
4.5a	Comparison of measured and computed deep water spectral transformation (data from May 5, 1976 at 16:15, case 3).	46
4.5b	Comparison of measured and computed deep water spectral transformation (data from May 11, 1976 at 10:15, case 6).	46
4.6	Wave transformation in finite depth water, the solid curve is the measured spectrum, dashed curve denotes the measured spectrum inshore and the dot dashed curve is the computed spectrum inshore using the solid curve as input.	47
4.7	Depth-limited significant wave height, H_ℓ, as a function of water depth and cutoff frequency.	50
4.8	Variation of wave height with square root of depth, 25 October 1980, Duck, North Carolina.	51
4.9	Comparison of numerical computations of shoaling waves obtained from the System 21 Mark 8 model (Abbott et al., 1978) in a one-dimensional mode, with the experimental results of Madsen and Mei (1969) labelled CERC Experiments.	54
4.10	Comparison of numerical results with measurements from a physical model.	55
5.1	Maps of the Beaufort Sea (a) and Sable Bank (b) showing the areas where bathymetric modification of waves takes place.	58

1. INTRODUCTION

Modern wave climate analysis relies increasingly on hindcasting techniques for estimation of extreme wave conditions. In circumstances where measured wave data are lacking, or available only for a few seasons, the usually much longer meteorological record is used to generate waves for a selection of historical storms and hence to provide synthetic data for extreme analysis. The current practice in wind-wave hindcasting (Resio, 1981; Sand et al., 1982; Greenwood et al., 1982) makes use of a discrete directional energy spectrum to describe the wave field. These models are not directly applicable to shallow nearshore areas for two reasons. First, the grid scale on which the wind forcing and the wind waves are discretized is often too coarse to resolve the features of interest. Secondly, wave hindcasting models have not been satisfactorily extended to account for refraction and energy dissipation in shallow water.

What is then needed for a reliable shallow water wind wave hindcast model is a system which will take as input the waves generated by a deepwater model (specified by a directional spectrum) and relate them to nearshore wave conditions by taking into account geometrical refraction and shoaling as well as energy dissipation. This kind of system should also be capable of including the sheltering effect of islands and peninsulas on the wave climate. Examples of locations in Canadian waters where shallow water hindcast models would be required include Sable Island and the Beaufort Sea.

This report first reviews recent research on the transformation of wave spectra from deep to shallow water. Application of refraction and shoaling methods to spectral evolution will be considered in Chapter 2 and what is known about various wave dissipation mechanisms in shallow water is presented in Chapter 3. The status of shallow water refraction and spectral wave modelling will then be discussed in Chapter 4.

Finally, in Chapter 5 the problem of modelling wind-waves from the scale of storms down to nearshore conditions is considered, and a practical modelling approach based on conventional deep water models and a spectral refraction procedure is recommended and discussed.

2. SHOALING AND REFRACTION

2.1 Plane Waves

As waves propagate from deep water into shallow water they are modified by interaction with the seabed. Even if we ignore processes which might increase (through wave generation) or decrease (through dissipation or reflection of waves) the energy flux in shallow water, modification of the wave energy can occur through convergence or divergence of this energy flux. This section deals with such processes.

Once the water depth becomes less than about a half of a wavelength, the velocity of wave crests (the phase velocity, c) and of the wave energy (the group velocity, V) becomes depth-dependent. Thus an initially straight wave front propagating into water of varying depth will become curved in a manner directly analogous to the refraction of light waves. In fact the first water wave refraction diagrams were produced using Huygen's principle to construct wave fronts, though direct plotting of wave rays (lines everywhere perpendicular to wave fronts) quickly became the preferred method. The wave ray equations, given, for example, by Munk and Arthur (1952), are

$$\frac{dx}{ds} = \cos\theta; \quad \frac{dy}{ds} = \sin\theta$$

$$\frac{d\theta}{ds} = \frac{1}{c}\left[\sin\theta \frac{\partial c}{\partial x} - \cos\theta \frac{\partial c}{\partial y}\right] \qquad (2.1)$$

where ds is an infinitesimal increment of the wave ray length, x,y are the two horizontal axes, and θ is the angle the ray makes to the x direction.

There are two ways in which wave energy changes along wave rays have traditonally been calculated. If we ignore generation or dissipation of wave energy the flux of energy between two rays must remain constant as the waves propagate. Thus

$$EVb = E_o V_o b_o \tag{2.2}$$

where E is the wave energy per unit surface area, b is the distance between rays and the subscript o refers to deep water conditions. Thus the proportional change in wave height, H, from deep water to any shallow water point can be written

$$\frac{H}{H_o} = \left(\frac{E}{E_o}\right)^{\frac{1}{2}} = \left(\frac{V_o}{V}\right)^{\frac{1}{2}} \left(\frac{b_o}{b}\right)^{\frac{1}{2}} = K_s K_r \tag{2.3}$$

where K_s is the shoaling factor and K_r is the refraction factor. For parallel bottom contours $K_r = \cos\theta_o/\cos\theta$. As an alternative to this procedure Munk and Arthur (1952) derived an ordinary differential equation for K_r along a single ray, without the need to compute two ray paths.

Both techniques have been widely used for monochromatic waves. Wilson (1966) gives computer programs for plotting wave rays and Aranuvachapun (1977) uses her program to show comparison between observed K_r values in the North Sea and those computed from ray separations. Skovgaard et al. (1975, 1976) also describe a computer wave refraction program and include wave dissipation effects due to bottom friction. Griswold (1963) discusses computer implementation of refraction diagrams and refraction coefficients by the Munk and Arthur method providing both continuous and finite difference solutions for K_r. Abernethy and Gilbert (1975) present a method of ray tracing based on triangular grid elements.

2.2 Refraction by Current

Waves are also refracted by currents, and this may be important in shallow water. Skovgaard and Jonsson (1977) show that the equations for the wave orthogonals (called rays in the discussion above) are unchanged provided the phase

velocity is replaced by the absolute velocity

$$c_a = c + U \cos\phi$$

where U is the current speed and ϕ is the angle between the current direction and the wave propagation direction. However they also point out, following Johnson (1947), that the direction of energy propagation is not the same as the wave orthogonal direction, except in the special case of co-linear waves and currents. They give a new set of equations for the energy propagation paths (called by them the wave rays). Calculation of the wave height or wave energy is much more difficult when currents are present since energy is exchanged between the waves and the current. Jonsson and Wang (1980) discuss equations appropriate for depth-current refraction, based on wave action and radiation stress concepts and give some solutions for idealized cases. Tayfun et al. (1976), following Phillips (1977), Willebrand (1975) and others make similar calculations for wave spectra. Noda et al. (1974) developed a rectangular grid finite difference scheme for studying monochromatic wave-current interactions in the nearshore zone. However the wave-current interaction equations are complex and have not been routinely used in practical refraction calculations. This may be a significant limitation on the accuracy of refraction models presently in use since there is some evidence for substantial wave-current interaction effects in some locations (Johnson, 1947; Smith, 1976; Hayes; 1980).

2.3 Refraction of Wave Spectra

Calculations of the refraction of wave spectra are generally based on the assumption that the wave energy flux in a frequency band of width df centred at frequency f remains in that band as the waves propagate; i.e. non-linear interactions which might transfer energy from one frequency to another are ignored. With this assumption it is possible

to calculate spectra in any depth of water (in the absence of currents and generation/dissipation processes) by dividing an initial spectrum into discrete frequency bands, refracting each frequency band separately and then recombining to form the refracted spectrum (Pierson et al., 1953, 1955). However the continuum of frequencies present in a spectrum requires that a subtle but important modification be made to equation (2.3). If $S(f,\theta)$ is the spectral energy density at frequency f for waves travelling in direction θ, then the transformation from deep water is given by

$$S(f,\theta) = S_o(f,\theta_o)\ K_s^2 K_r^2\ \frac{\partial\theta_o}{\partial\theta} \qquad (2.4)$$

The additional term, $\partial\theta_o/\partial\theta$, is a Jacobian allowing for the change of the angle variable θ from deep to shallow water (Pierson et al., 1953; Dorrestein, 1960; see also LeMéhauté and Wang, 1982).

One important effect of this additional term is the removal of 'caustics' present in the monochromatic results. Caustics will occur when wave rays cross each other. Since b becomes zero at a crossing, equation (2.3) predicts an infinite wave height at that point. However in a continuum of frequencies there is infinitesimal energy associated with a caustic for any given frequency and the integrated energy over a finite bandwidth remains finite. In equation (2.4) K_r tends to infinity as a caustic is approached but the Jacobian term tends to zero since the direction is not unique for a given deep water direction. Thus the product of these terms remains finite (Dorrestein, 1960).

The first rigorous theoretical approach to the evolution of spectra in shallow water is due to Longuet-Higgins (1956, 1957). He showed the surprising result that the energy density, if defined per unit area of wave number space, remains constant along a wave ray. Karlsson (1969) showed

that this is equivalent to the conservation equation, for $S(f,\theta)$, the energy density in (f,θ) space,

$$V C S(f,\theta) = V_o C_o S_o(f_o,\theta_o)$$

or, since the frequency also remains constant as the waves propagate,

$$S(f,\theta) = \frac{V_o}{V} \frac{k}{k_o} S_o(f,\theta_o) \qquad (2.5)$$

where k is the wave number (2π/wavelength). Dorrestein (1960) and LeMéhauté and Wang (1982) show that this is equivalent to equation (2.4). Collins (1972) generalizes this to the case where dissipation or generation are included, and Phillips (1977, page 182) gives a related equation when currents are included.

For the special case of straight parallel bottom contours Krasitskii (1974) gives analytic solutions to equation (2.5). He applies his theory to refract a deep water Pierson-Moskowitz spectrum into shallow water. Collins (1972) solves the same special case numerically and is able to include dissipation and generation.

2.4 Computational Methods

Two numerical schemes have been developed to solve equation (2.5) for three-dimensional bathymetry. Collins (1972) first constructs wave rays in the conventional way and then can apply equation (2.5) along each ray; when generation and dissipation effects are being included this involves numerical integration along the ray path. Shiau and Wang (1977) on the other hand solve the ray equations and equation (2.5) on a square grid. Their seaward boundary is either taken out to deep water or, since this generally involves excessive computation time, bottom contours are assumed to be straight and parallel seawards of their model boundary and

Krasitskii's (1974) analytical solutions are used to bring deep water spectra to their seaward boundary.

LeMéhauté and Wang (1982) compare these recent schemes with the more traditional 'heuristic' calculations based on equation (2.4). They conclude that in general equation (2.5) is much simpler to use since k and V depend only on depth and frequency, and not on angle of approach. However all methods require a refraction diagram, or its equivalent (though this will be simple to obtain for straight parallel contours). They remark that, since such a refraction diagram is required even to compute the one-dimensional spectrum $S(f)$, complete determination of $S(f,\theta)$ should not require much additional work.

Whatever the method used to compute refraction diagrams, it is important to recognize the limitations inherent in such computations. Firstly, since the wave amplitude calculations are independent of the ray path calculations, there are no constraints on along-crest amplitude variations as waves refract. Where these along-crest amplitude variations become large, diffraction effects come into play to smooth out the variations. For monochromatic waves the problem is particularly acute due to the prediction of caustics. Computer programs to model both refraction and diffraction of monochromatic waves have been developed by Berkhoff (1973, 1975) and by Chen and Mei (1974), and studies, both theoretical and experimental, of diffraction over idealized topography form an active area of research at present (see for example Jonsson et al., 1976; Meyer, 1979; Lozano and Liu, 1980). Results generally suggest that wave amplitudes at caustics are amplified only by factors of 2 or 3. However computation of diffraction effects is currently very expensive and is not a routine operational procedure. There does not appear to have been any attempt to consider diffraction effects in wave spectra.

An alternative to a full calculation of diffraction is to smooth refracted waves over some spatial region or grid of sub-regions. Bouws and Battjes (1982) suggest a version of such a procedure and remark that it should also reduce the sensitivity of the calculations to schematization of the bathymetry and to numerical procedures. In their procedure, which they call a Monte Carlo approach, the refraction coefficient (equation 2.4) is ignored, and the total energy in a given sub-region or 'bin' is simply the sum, over all rays passing through the sub-region, of the product of ray energy and the time that it takes the ray to traverse the sub-region. Summation is over all incident angles of approach and may include summation over discrete frequencies too. In the spirit of a statistical sampling scheme, they treat the uncertainty in their estimates as a compromise between confidence and resolution, the latter including both frequency space and physical space. Qualitative comparisons are made with data from the JONSWAP array, and suggest that the scheme provides useful results. Further discussion of these points is presented under "caustics" (4.1.2) below.

2.5 Nonlinear Wave Refraction

The refraction of finite amplitude waves has been studied by, among others, Ryrie and Peregrine (1982). The results show that linear theory does a good job of estimating wave angle until very close to the break point, except for waves travelling almost parallel to depth contours. Waves travelling within about 25 degrees of the contours may, depending on the wave amplitude, be refracted in a direction opposite to that of linear waves, an unexpected phenomenon which the authors term 'anomalous refraction'. Since there do not appear to be any field observations of this effect it is not clear that it is important in practice. In fact, since the effect is only important at relatively large values of off-shore steepness (deep water wave height to wavelenghth ratios greater than about 0.04), it may be unimportant for

a spectrum of waves continuous in both frequency and direction of approach. Nevertheless Ryrie and Peregrine are continuing work on this effect and its practical relevance should become clearer.

Ryrie and Peregrine's (1982) results also show that linear wave theory predicts wave height remarkably well until very close to the break point, at least on their linear, parallel bottom topography. Thus, for example, even for a deep water wave steepness of about 0.1, wave heights calculated by their 'numerically exact' calculations are less than 5% higher than linear theory until the depth reduces to 1.5 times the breaking depth. As discussed above, many of the details of the wave spectra will be modified in much deeper water, but, for many practical purposes for which wave height is the critical parameter, linear theory seems to be quite adequate into very shallow water.

However the finite amplitude theories do diverge substantially from linear theory in prediction of wave heights and directions at the point of breaking. Both Ryrie and Peregrine (1982) and Petersen (1977) (the latter using cnoidal wave theory) agree that nonlinear waves are higher at breaking and are refracted less than linear waves. The effects are greatest for the steepest offshore waves, of course. Breaker heights can be up to twice linear theory predictions and a 30% difference in wave angle can occur in the case of cnoidal waves. Again, however, the relevance of this to spectra of incoming waves is not yet clear. Certainly the comparisons of Bryant (1979) suggest that linear wave theory is adequate for predicting breaker height (Figure 2.1); there is no obvious systematic deviation from linear theory, though the results are very scattered. Skovgaard et al. (1976) suggest calculating the Ursell number (HL^2/h^3, where H is wave height, L is wavelength and h is water depth) along rays in their wave refraction program, and

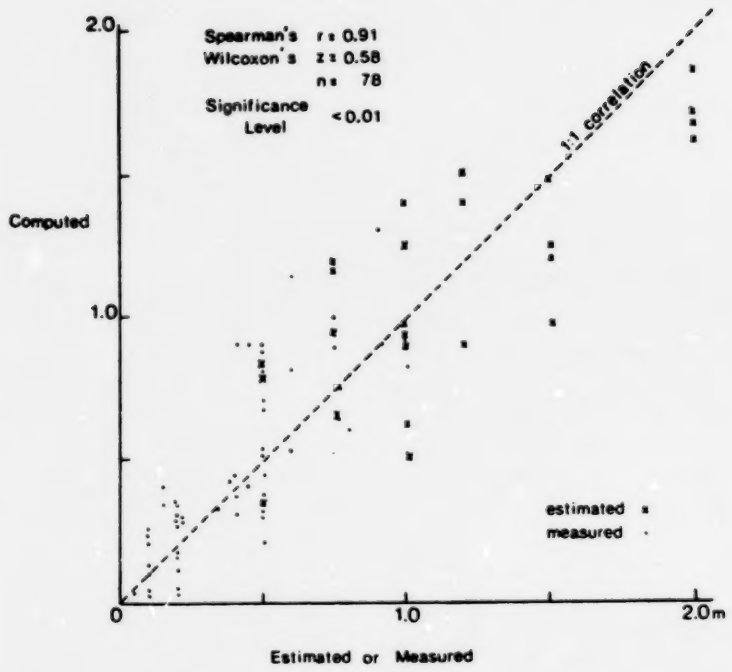

Figure 2.1 Comparison of observed and computed breaker wave heights, Broken Bay, Australia. From Bryant (1979).

changing to nonlinear equations once this number gets larger than say 10 or 20. However it is far from obvious that this is relevant for a spectrum of incident waves.

3. DISSIPATIVE PROCESSES

Observations of shallow water waves indicate that in addition to the geometrical effects of shoaling and refraction discussed in Chapter 2 there is a significant amount of energy loss due to a variety of mechanisms, such as bottom friction, seepage and wave breaking. These processes can play an important role in determining the form and the level of the nearshore wave spectrum. We shall review the main dissipation mechanisms as well as effects such as nonlinear interactions which may transfer energy between parts of the spectrum in this chapter.

3.1 Boundary Layer Friction

Shear stresses at the boundary between a rigid bottom and the fluid above it may be expressed as (Putnam and Johnson, 1949)

$$\underset{\sim}{\tau} = \rho C_f \underset{\sim}{u}|\underset{\sim}{u}| \tag{3.1}$$

(some authors such as Kamphuis (1975,1978) and Jonsson (1966) use $\tau = \frac{1}{2} \rho C_f \underset{\sim}{u}|\underset{\sim}{u}|$), where $\underset{\sim}{\tau}$ is the bottom shear stress, ρ the water density, C_f a friction coefficient and $\underset{\sim}{u}$ the velocity just above the boundary layer. There is in general a phase lag between $\underset{\sim}{\tau}$ and $\underset{\sim}{u}$ and this may be taken into account when calculating the rate of energy dissipation in the bottom boundary layer: (Jonsson, 1966; Hasselmann & Collins, 1968; Jonsson and Carlsen, 1976)

$$\frac{\partial E}{\partial t} = < \underset{\sim}{\tau} \cdot \underset{\sim}{u} > \tag{3.2}$$

where E is the wave energy density and the angled brackets represent an average over a wave cycle.

This dissipation mechanism is by far the best studied; it has been investigated in the laboratory and applied to explain the attenuation of shoaling waves in the field in a

number of instances. In the majority of cases studied, the bottom friction model provides a satisfactory account of wave attenuation.

Most field measurements (Bretschneider and Reid, 1954; Hasselmann and Collins, 1968; Iwagaki and Kakinuma, 1963; Shemdin et al., 1978; Hasselmann et al., 1973; Hsiao and Shemdin, 1978) yield values of C_f ranging from 0.008 to 0.05. A representative value of $C_f \simeq 10^{-2}$ has often been used. Larger values have however been found: Van Ieperen (1975) computed $C_f \simeq 0.06$ to 0.10 offshore of Melkbosstrand, South Africa.

Why is there such a wide range of observed values of C_f? Or, to reword the question slightly, why is such a wide range of values of C_f necessary to fit observed wave attenuation through the bottom friction model? This question has been addressed in a variety of ways.

In a series of laboratory experiments, Jonsson (1966), Iwagaki et al. (1965), Jonsson and Carlsen (1976), and Kamphuis (1975,1978) have sought to establish, under controlled conditions, relations between the friction coefficient C_f and parameters specifying the flow or the bottom roughness. Tests were performed for a range of values of a bottom roughness parameter (a/K_s, where a is the horizontal particle displacement associated with wave motion and K_s = twice the sand grain diameter) and of the Reynolds number ($R = |\underset{\sim}{u}|a/\nu$, with ν the kinematic viscosity). Results, summarized in Figure 3.1, indicate that as the flow passes from the laminar to an increasingly rough turbulent regime, the friction factor varies by more than two orders of magnitude.

Furthermore, it has been noted that when sand ripples are present, bottom friction is enhanced due to form drag: the additional energy dissipation occurs in the vortices formed

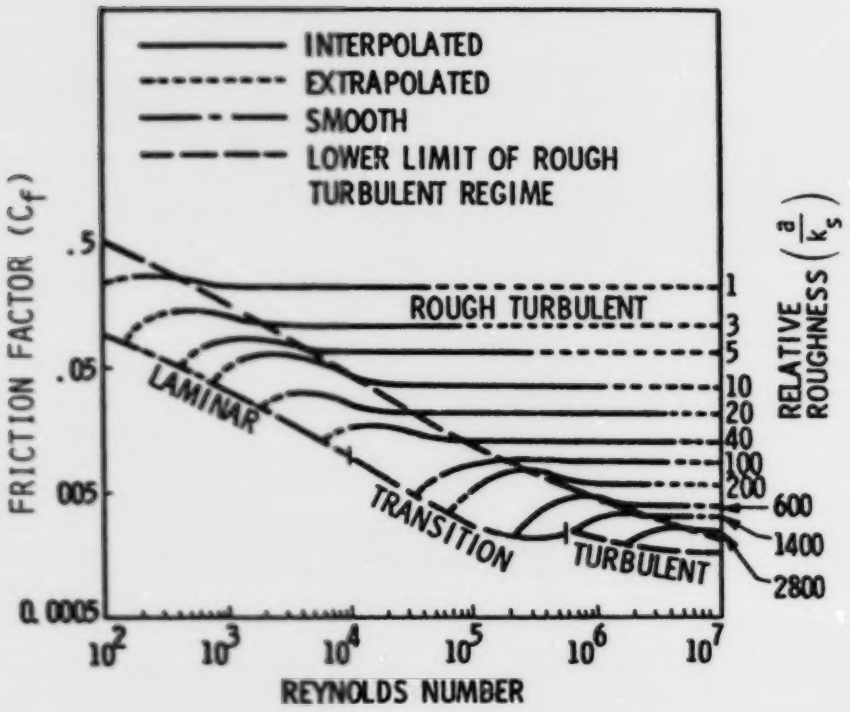

Figure 3.1 Friction factor diagram showing the variation in C_f with Reynolds number and bottom roughness for a rigid bottom (after Kamphuis, 1978).

above the ripple troughs. Ripple formation has been reviewed by Dingler (1975) and Nielsen (1977). Bottom stress in the presence of ripples has been found to be strongly dependent on their steepness (Dingler, 1975; Turnstall and Inman, 1975), as shown in Figure 3.2.

Clearly then the specification of an appropriate value of C_f to model wave damping in the bottom boundary layer requires some knowledge of bottom sediments, in particular as to the presence and character of ripples.

In addition C_f depends, through its dependence on the Reynolds number, on the local wave height. For uniform bottom properties, for example, C_f would vary shorewards because of shoaling according to Figure 3.1.

Finally, the velocity $\underset{\sim}{u}$ which enters equations (3.1) and (3.2) is related to the wave amplitude through a model of the wave motion. Most applications use a linear model; Isaacson (1977) has used a higher approximation in wave amplitude, finding somewhat higher attenuation rates. As shoaling waves rapidly distort beyond the linear profile, this point is also of some relevance.

Since the nonlinear bottom friction depends upon the total velocity field, and not on particular frequency or direction components of the velocity field, its parameterization poses problems for ray-following techniques of calculating the transformation of spectra. In principle all possible rays are needed at all points to enable the quadratic bottom dissipation to be accurately modelled. For this reason, Collins (1972) proposes a simplification of the Hasselmann and Collins (1968) bottom friction parameterization in which the ratio of the total energy at any point along a ray to that in deep water is assumed to be equal to the ratio of

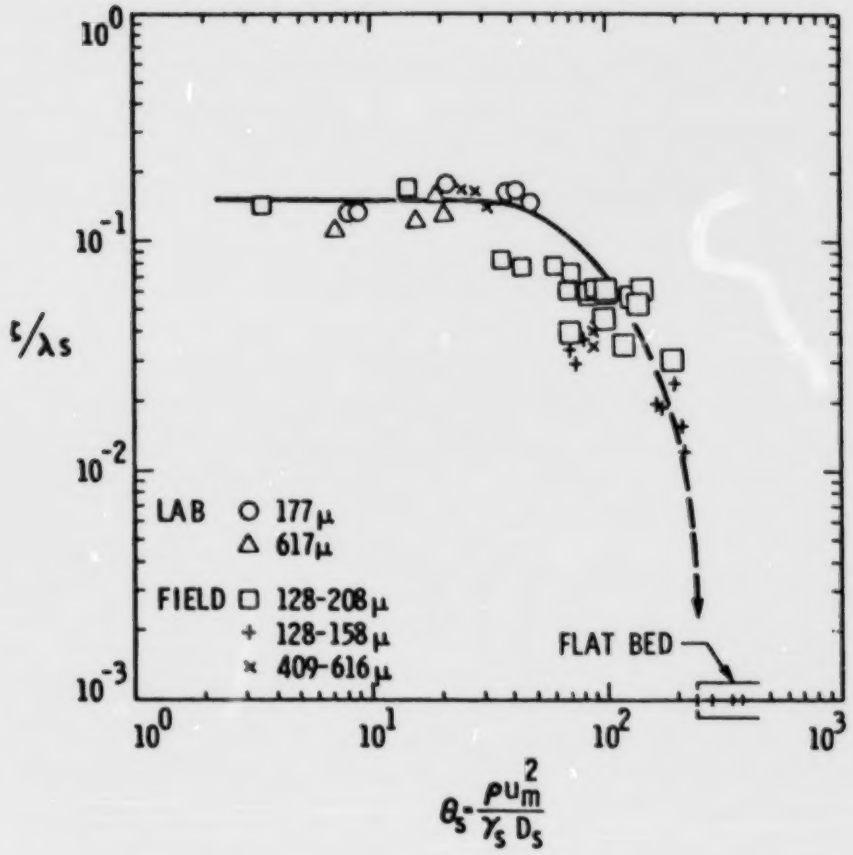

Figure 3.2 Ripple steepness ζ/λ_s, against dimensionless bottom stress θ_s. This is the equilibrium stress which will destroy ripples of the given steepness. ζ and λ_s are ripple height and length respectively; u_m is the wave particle velocity above the ripples, D_s the mean sand grain diameter, $\gamma_s = (\rho_s - \rho)g$ with ρ the water and ρ_s the sand density. (After Dingler, 1975).

local to deep water $S(f,\theta)$ values associated with the ray. He remarks that this underestimates the energy loss by bottom friction, and this may explain the tendency of his predictions to overestimate the spectra. Cavaleri and Rizzoli (1981), also using a ray technique, estimate the local energy from a parametric model based on the mean JONSWAP spectrum computed for the local wind and dimensionless fetch at each point along the ray. Presumably this problem with parameterization of the bottom friction is not as acute in grid models of refraction. Wang and Yang (1981) include bottom friction in some of their calculations, but do not give details of their procedure.

3.2 Percolation

Wave dissipation through percolation is associated with seepage of fluid, under varying wave pressures, through porous sediments, with subsequent dissipation of the energy by friction against the sediment matrix. Percolation provides significant damping for sands with diameters above $D \tilde{=} 0.4$ mm.

Putnam (1949) first calculated wave attenuation due to percolation. A more general (and corrected: Putnam having overestimated the dissipation by a factor of 4 due to an arithmetic error) result was obtained by Shemdin et al. (1977):

$$\frac{1}{E}\frac{dE}{dt} = -k\sqrt{\alpha\beta}\,\frac{\tanh\sqrt{\frac{\alpha}{\beta}}\,kd}{\cosh^2(kh)} \qquad (3.3)$$

where E is the energy density, k the wave number, h the water depth, d the thickness of the sand layer and α and β the horizontal and vertical coefficients of permeability respectively. This result is also based on linear wave theory. Figure 3.3 compares dissipation rates for various mechanisms and shows that percolation in coarse sand may be more important than bottom friction in deep water.

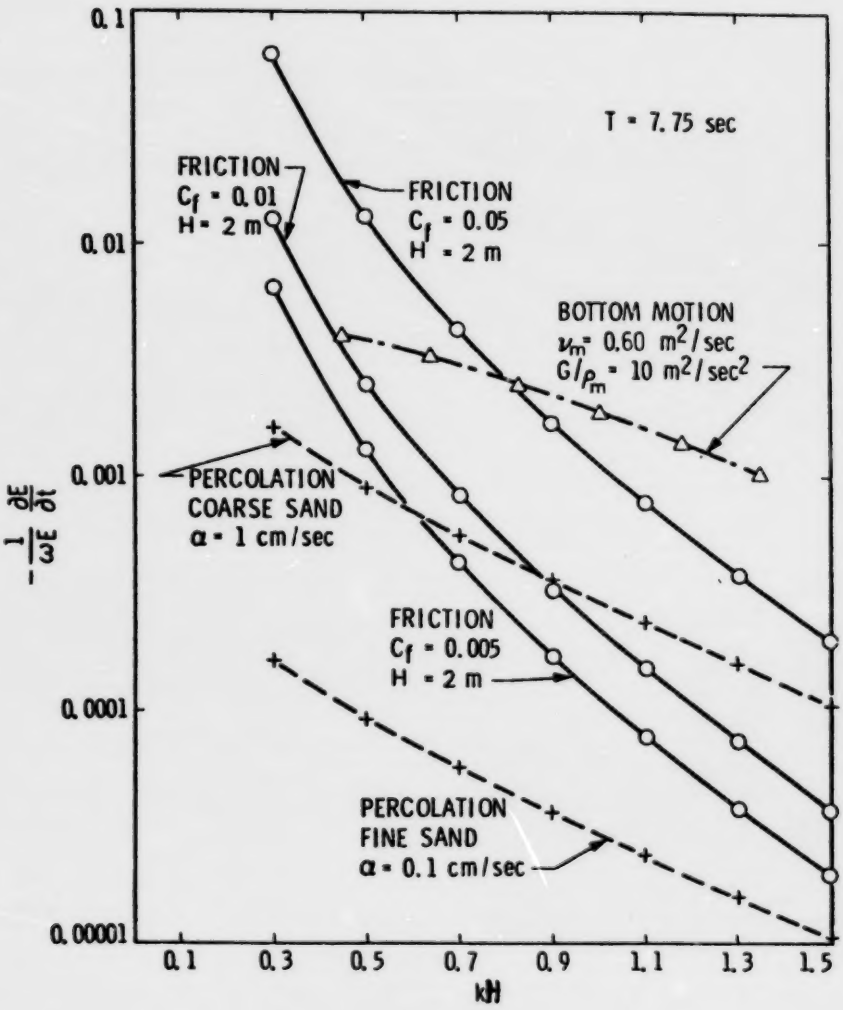

Figure 3.3a Comparison between dissipation mechanisms. H is the water depth, $\alpha=\beta$ the porosity of the isotropic sediments (cf. equation 3.3), G the shear modulus and ρ_m the density of mud. Bottom motion attenuation is based on the model of Hsiao and Shemdin (1980). The abscissa $(-\partial E/\partial t/E\omega)$ is the proportional rate of energy loss per period. (After Shemdin et al., 1977).

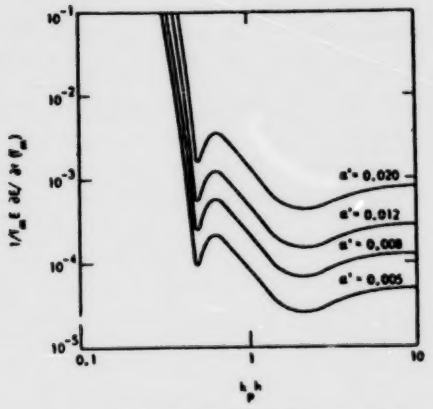

WAVE - WAVE INTERACTION TRANSFER RATE AT THE SPECTRAL PEAK AS A FUNCTION OF THE EQUILIBRIUM RANGE LEVEL α'.

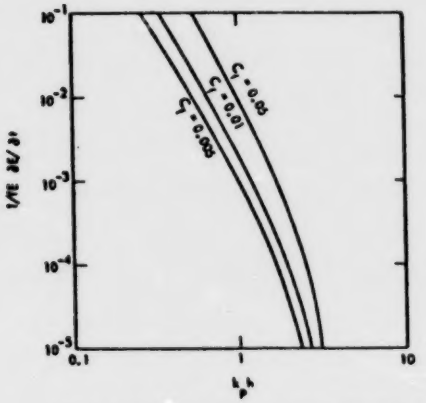

ENERGY DISSIPATION RATE DUE TO FRICTION AS A FUNCTION OF C_f. THE DISSIPATION RATE ALSO DEPENDS ON WAVE HEIGHT, H AND PERIOD, T (H=2.0m AND T = 7.75 s USED IN THIS FIGURE).

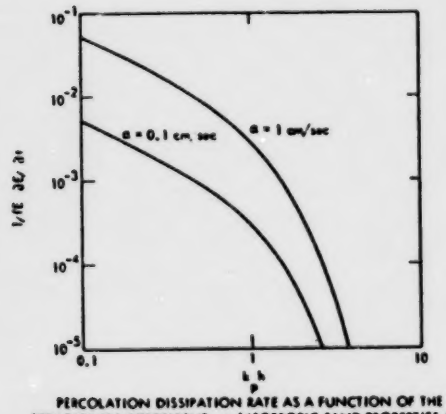

PERCOLATION DISSIPATION RATE AS A FUNCTION OF THE PERMEABILITY COEFFICENT, a (ISOTROPIC SAND PROPERTIES ARE ASSUMED). THE DISSIPATION RATE ALSO DEPENDS ON WAVE PERIOD, T (T = 7.75 s USED IN THIS FIGURE).

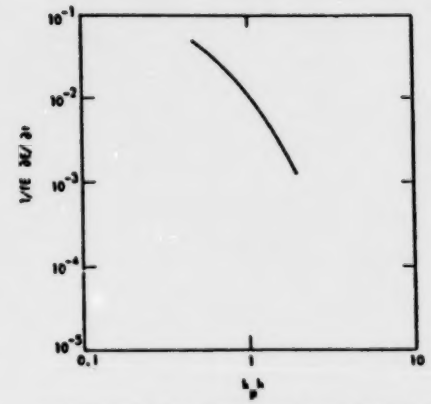

BOTTOM MOTION DISSIPATION RATE FOR MUD VISCOSITY $\nu = 0.6\ m^2/s$, RATIO OF MUD SHEAR MODULUS TO DENSITY $G/\rho = 10\ m^2/s^2$, MUD THICKNESS = 3 m, AND WAVE PERIOD = 7.75 s.

Figure 3.3b Relative significance of wave transformation mechanisms as a function of $k_p h$, where k_p is the wave number at the peak of the deep water spectrum and h the depth. From Shemdin et al. (1980).

3.3 Bottom Motion

Very high rates of wave attenuation have been observed in areas of soft muddy bottoms. Gade (1958) mentions a near-shore location in the Gulf of Mexico, known as the Mud Hole, where wave attenuation is so high that fishing boats use it as an emergency harbour during storms. Bea (1974) and Tubman and Suhayda (1976) also reported very rapid attenuation of waves near the Mississippi delta. MacPherson and Kurup (1981) have also reported strong damping of waves over the Kerala mud flats. The enhanced energy dissipation is attributed to strong coupling of water waves with the unconsolidated bottom muds which are set into a wave motion of their own.

A number of theoretical models have been put forward to represent the wave-sediment coupling based on various rheological relationships for the sediment behaviour. Gade (1958) considered a viscous Newtonian mud layer underlying the sea and found realistic dissipation rates. This model was extended by Dalrymple and Liu (1978) to include a wider range of wave lengths. More complex rheologies, based on measured properties of marine sediments (Carpenter et al., 1973; Hamilton, 1979) included elastic effects (Mallard and Dalrymple, 1977)--which by themselves were found not to lead to any damping; visco-elastic media (Hsiao and Shemdin, 1980); porous media (Hunt, 1959; Liu, 1973) and poro-elastic studies of various kinds (Rosenthal, 1978; Yamamoto et al., 1978; Madsen, 1978; Yamamoto, 1982).

Most of the models which include internal friction in the sediments can account for the rapid attenuation rates observed over muddy bottoms (Figure 3.3). Laboratory experiments described by Yamamoto (1982) yield reasonable agreement between his poro-elastic theory and observed attenuation rates (Figure 3.4).

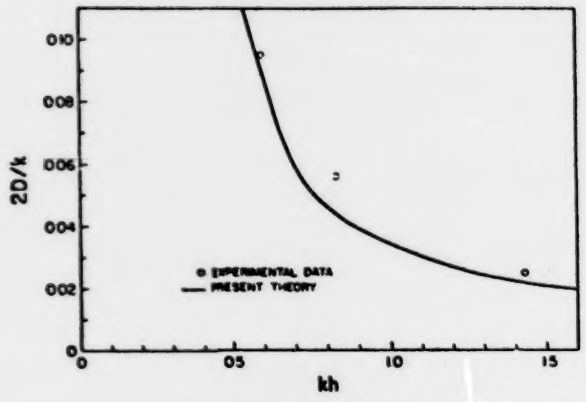

Figure 3.4 Comparison of Yamamoto's (1982) damping theory with laboratory data. k and D are respectively the real and imaginary parts of the wave number, h is the water depth. From Yamamoto (1982).

It is thus clear from the above that an estimate of wave attenuation requires not only knowledge of the form and roughness of the ocean bottom, but also of its rheological properties. Soft clay bottoms in particular induce rapid wave damping. Table 3.1 (from Yamamoto, 1982) gives estimates of damping rates for three types of bottom sediments in different water depths.

3.4 Back Scattering

Waves travelling in shallow water may be scattered by bottom irregularities. Although the total wave energy remains conserved in this process, the shoreward energy flux will be reduced by the fraction of energy scattered in the offshore direction. Long (1973) has explored this mechanism for the JONSWAP area (Hasselmann et al., 1973) and found it potentially important. Later measurements by Richter et al. (1976) suggest that with the observed bottom irregularities, scattering is inadequate to explain the observed attenuation. This mechanism remains poorly explored and has yet to be applied to other areas. One might expect for example that it could be important in the presence of regularly spaced sand bars or other large underwater features, as indeed Lau and Barcilon (1972) and Lau and Travis (1973) have found by theoretical analysis.

3.5 Finite Amplitude Effects

The wave spectrum is only a good descriptor of the wave field if the different frequency components making up the spectrum are essentially independent. For most ocean depths this is a fair approximation, despite the fact that nonlinear exchanges of energy across frequency bands are known to be a vital part of wave generation and dissipation. Most schemes for modelling transformation of spectra in shallow water therefore assume that energy in a particular frequency band stays in that frequency band as the spectrum propagates.

Table 3.1

Exponential damping coefficients D [wave amplitude proportional to exp(-Dx)] for waves of period T = 15 s, height H, length L and group velocity c_G in various water depths h and for three types of sediments. From Yamamoto (1982).

		Location			
		h = ∞	h = 70 m	h = 50 m	h = 30 m
Sand bed	H	24.0	21.8	21.7	21.3
	L	351.0	311.0	276.8	233.6
	c_G	11.7	14.0	13.8	13.0
	D	0	4.13×10^{-6}	8.03×10^{-6}	1.53×10^{-5}
Silty clay bed	H	24.0	1.5	1.1	0.8
	L	351.0	307.3	278.9	226.1
	c_G	11.7	13.8	14.3	13.9
	D	0	7.60×10^{-4}	1.40×10^{-4}	1.79×10^{-4}
Soft clay bed	H	24.0	9.9	1.7	0.1
	L	351.0	342.1	334.3	214.0
	c_G	11.7	13.0	16.5	13.9
	D	0	4.16×10^{-4}	8.69×10^{-4}	1.18×10^{-3}

However it is well known that wave forms change as waves shoal, the ultimate manifestation of this being breakers approaching a shoreline. In a spectral sense this wave form transformation implies that energy is being transferred into different frequency bands, and different frequencies are no longer independent.

One effect of this 'nonlinear interaction' which has frequently been observed in laboratory and numerical experiments is wave splitting. Finite amplitude waves evolve as they propagate and a single wave may split into two or more waves. Madsen and Mei (1969), for example, show theoretical and experimental evidence for the splitting of solitary waves as they propagate over an uneven bottom. Even over constant or very slowly varying depths finite amplitude waves change shape as they propagate and may show a continuously varying sequence of wave forms which repeats over a 'repetition length' (e.g. Benjamin, 1974). Observations show the often spectacular, but very local, generation of secondary waves as waves propagate over a reef or sand bar (e.g. Gallagher, 1972). The relevance of these phenomena to wave spectra in general is not yet clear. An illustration of possible wave splitting is shown in Figure 3.5. Observations at Port Elgin, Ontario (Baird and Glodowski, 1977) show that peak periods inside the harbour never exceed 3 sec. while they reach up to 9 sec. outside. Whether this feature is due to wave splitting or to some type of period dependent attenuation remains unknown.

However an effect that is readily observed in the real ocean is the generation of harmonics of a spectral peak as waves travel into very shallow water. Shemdin et al. (1980) estimate that wave-wave interaction at a spectral peak becomes rapidly more important as $k_o h$ gets below about 0.5, where k_o is the wave number of the peak and h is the water depth (Figure 3.3b). As an excellent example of this interaction

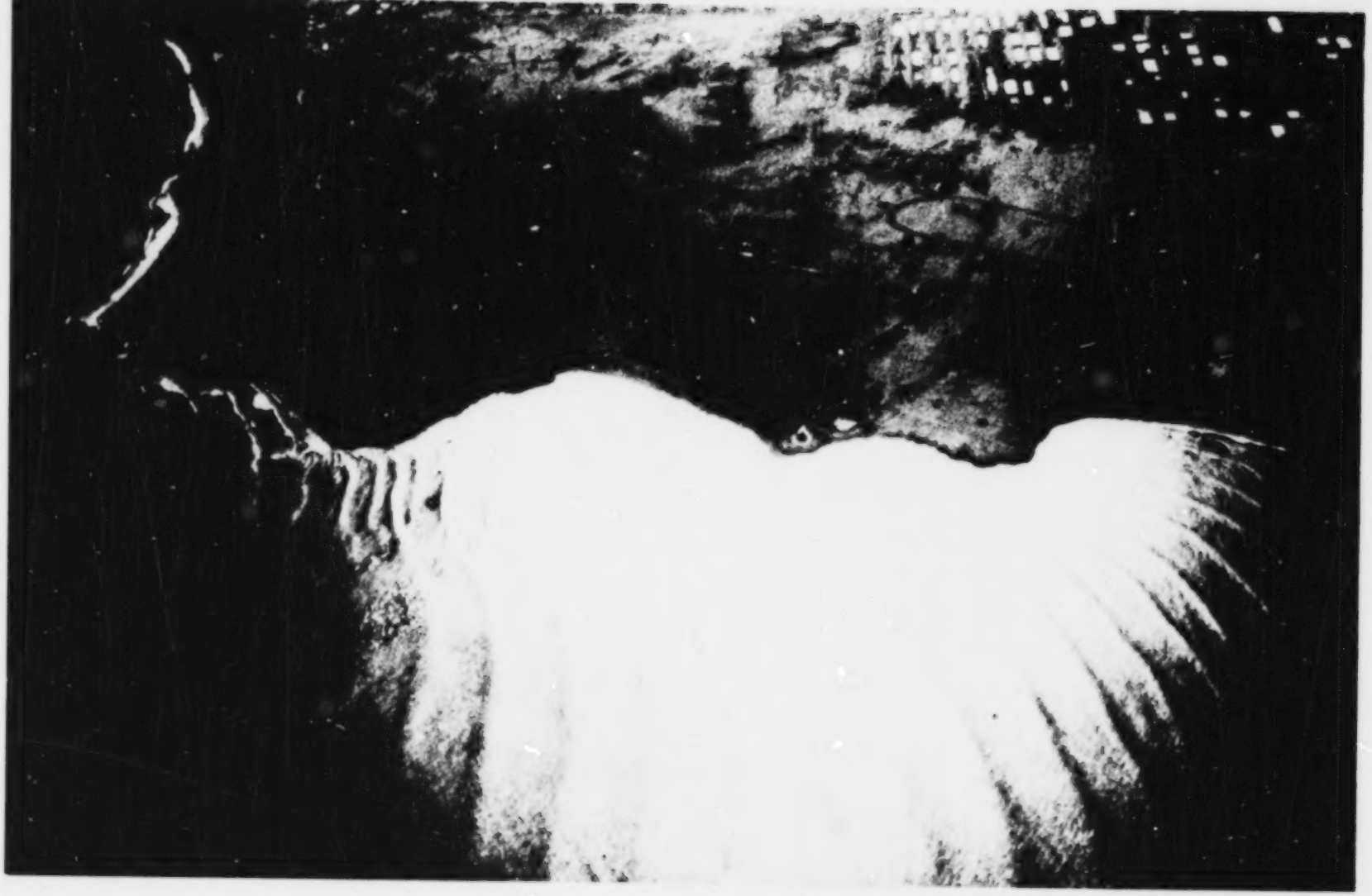

Figure 3.5 Photograph of regular waves refracting near a coastline, with possible wave splitting near the left-hand point (additional crests appearing between the regular wave crests next to the coast) (Photo courtesy of Dr. George L. Pickard).

interaction Guza and Thornton (1980) show the development of harmonic peaks in a spectrum as waves propagate from 10 m depth into 1.8m depth (Figure 3.6a) and show the inadequacy of linear shoaling and refraction theories in modelling this development (Figure 3.6b).

Freilich (1982) has modelled this nonlinear interaction using the Boussinesq equations. The incident spectrum was divided into discrete frequencies, with all possible 'nearly resonant' triad interactions allowed between them. Only normally incident waves were considered, propagating over a constant 2.2% bottom slope. The numerical scheme took measured spectra from 10 m depth and shoaled them to 3 m depth over a total distance of about 270 m. Comparisons were made with measured spectra at six sensors across this distance. An example of the results is shown in Figure 3.7. As might be expected, the nonlinear model was much better than a linear model for the shallow sensors and at high to mid frequencies. Interestingly the most prominent effect appeared in the phases of the waves at harmonic frequencies, where forced waves are more important than free waves. For broad-banded, low-energy conditions, and in relatively deep water, however, the linear approximation was quite satisfactory. Unfortunately the numerical calculations were very time consuming and hence very expensive. Freilich suggests that linear theory should be used for broad-banded, low-energy conditions, while for narrow band spectra non-linear calculations should be used for peak-peak-harmonic interactions but are probably not necessary at other frequencies. Unfortunately no attempt has yet been made to quantify the 'broad-banded' or 'low-energy' conditions, though work is continuing.

Hasselmann and Hasselmann (1980) have calculated numerically the nonlinear transfer due to third order wave-wave interactions in finite depth water for directional spectra.

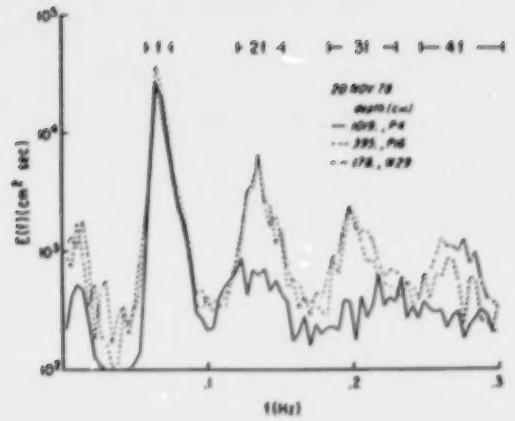

(a)

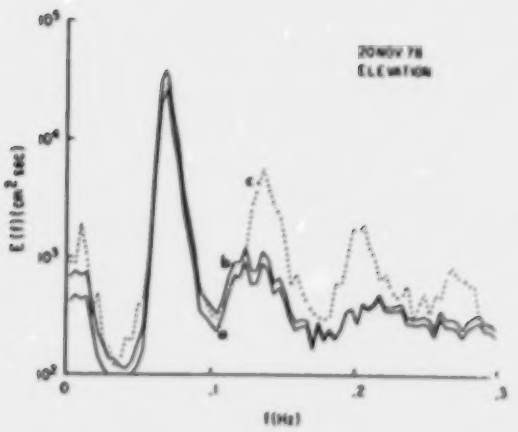

(b)

Figure 3.6 a) The generation of harmonics in shoaling waves; b) comparison between predicted and observed spectra. curve a is the elevation spectrum in 1019 cm depth; curve b is the predicted spectrum in 395 cm depth and curve c is the observed spectrum in 395 cm depth. From Guza and Thornton (1980).

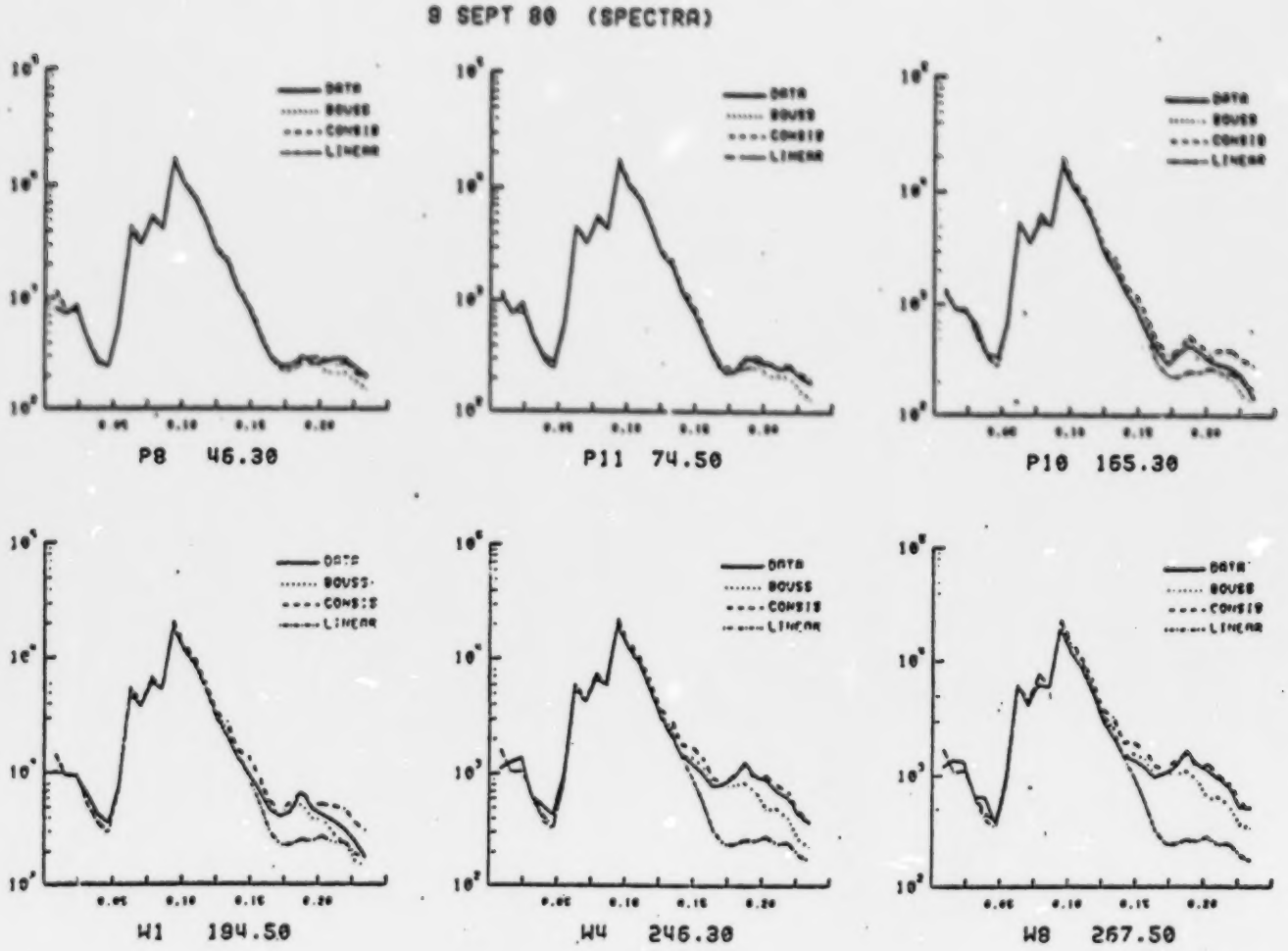

Figure 3.7 Comparison of power spectra between measured data ("DATA"), the Boussinesq model ("BOUSS"), another non-linear model used by Freilich ("CONSIS") and linear theory ("LINEAR"). The ordinate is frequency (Hz) and the abscissa is spectral density (cm^2/Hz). P and W represent pressure sensors & wave staffs respectively. The distances in metres, from the input sensor are also shown beneath each graph. From Freilich (1982).

Their calculations use JONSWAP spectra as input, and results show a very rapid increase in the importance of wave-wave interaction as the depth decreases (Figure 3.3b). Shemdin et al. (1980) use their calculations in a comparison with data obtained from the JONSWAP site, but the example considered, transformation from 17 m to 13 m over about 18 km, is not shallow enough to show strong influence of the wave-wave interactions.

3.6 Wave Breaking

Wave breaking takes place in deep water and limits the growth of the high frequency part of the spectrum. Phillips (1958) invoked dimensional arguments to derive an equilibrium range for wind waves in the range of frequencies above the spectral peak for which wave energy is limited by breaking. For the equilibrium range, the frequency spectrum $S(\omega)$ is given by

$$S(\omega) = \beta g^2 \omega^{-5} \qquad (3.4)$$

where β is a non-dimensional constant and g the acceleration of gravity. This power law dependence is frequently observed in well developed seas and has been incorporated in commonly used spectral representations such as the Pierson-Moskowitz or the JONSWAP spectra. Deep water breaking is thus already included in present wave hindcasting models explicitly, as in Hasselmann (1974) or implicitly in assuming some limiting spectral form.

In shallow water, waves break by overtopping where the ratio of wave height to undisturbed water depth reaches a certain value. This value may vary with breaker type (Bowen et al., 1968) but from theoretical considerations (Miche, 1944) should be around 0.78.

Breaking produces a marked decrease in the level of the peak of the spectrum; the distortion which precedes breaking leads to the appearance of harmonics of the spectral peak and to a relative increase in the importance of both high and low frequency (well above and below the spectral peak) parts of the spectrum. Examples of spectral changes due to breaking are shown in Figure 3.6 and 3.8. There is a tendency for a new high frequency equilibrium spectrum to re-establish itself, but it has been argued by a number of authors, starting with Kitaigorodskii et al. (1975) that the power-law dependence should be modified in shallow water to an ω^{-3} dependence, in agreement with measurements made by Dreyer (1973). A simple theoretical justification was advanced by Thornton (1977) who argued that if the wave speed c was taken as the variable responsible for breaking, the equilibrium range should obey (on dimensional grounds)

$$S(\omega) = \beta c^2 \omega^{-3}$$

In deep water, $c^2 = g^2/\omega^2$ and one recovers equation (3.4); in very shallow water, $c^2 = gh$ and the equilibrium range becomes

$$S(\omega) = \beta g h \omega^{-3}$$

The measurements made in shallow water by Dreyer (1973), Thornton (1976, 1977) and Vincent et al. (1982) confirm the goodness of fit of the ω^{-3} equilibrium spectral shape at high frequencies.

Following early work by Ijima et al. (1970), Sawaragi and Iwata (1980) have suggested that an extremely shallow water equilibrium range [with wave height/water depth $\leq$ 0.4] could exist, with $S(\omega) \propto \omega^{-1}$. In the presence of a return flow from backwash the dependence would be modified to ω^{-2}. Experiments in wave tanks, in water depths of a few centimeters have provided some confirmation for the presence of more than one equilibrium region, but these ideas have not been confirmed by field data.

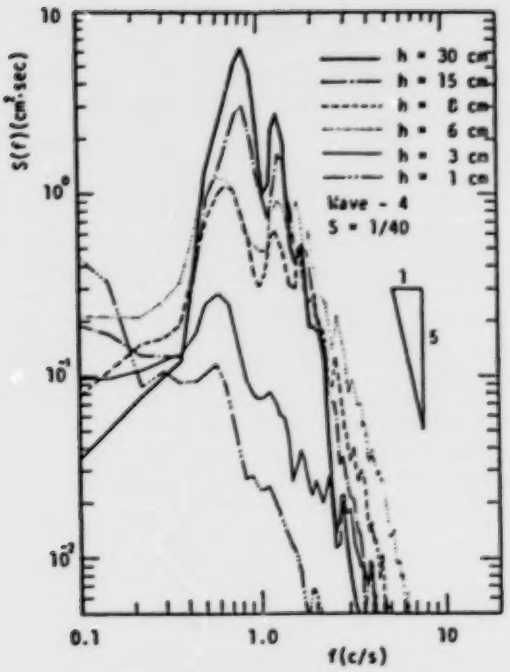

Figure 3.8 Wave spectrum change due to shoaling and breaking. From Sawaragi and Iwata (1980).

3.7 Wave Generation

Two mechanisms appear to be involved in the generation of waves by the wind. In the initial stages of wave growth the turbulent pressure spectrum generates waves whose phase speeds match the wind speed by resonant interaction. This mechanism, investigated by Phillips (1957), results in a linear growth of the wave spectrum. Once the waves grow to a certain size they influence the atmospheric turbulence themselves and wave growth becomes much more rapid, increasing exponentially (Miles, 1957). Both of these generation mechanisms have been parameterized in spectral transformation calculations (e.g. Collins, 1972; Cavaleri and Rizzoli, 1981) though there are some differences of detail. The forms used, however, are not appropriate to very shallow water where the waves are non-dispersive. Vincent et al. (1982) argue that their field spectra from between 36 m and 2 m water depth were significantly influenced by wave generation, and comment that, due to the absence of dispersion in shallow water, all parts of the spectrum may receive direct forcing by the wind even in depths as large as 17 m. If this is the case there is a clear need for more study of shallow water wave generation.

4. STATUS OF SHALLOW WATER WAVE MODELS

Just how well does the combination of ray tracing and wave damping reproduce nearshore conditions given deep water waves? We shall first take a critical look at some problems arising in refraction studies and then review the success of spectral modelling techniques in shallow water.

4.1 Factors Affecting the Accuracy of Ray Tracing

4.1.1 Parameterization of Depth

The computer refraction programs generally in use (Skovgaard et al. (1975) review several examples) require depths to be specified at grid points over the region of interest. The programs then employ some method of interpolation to find depths along ray paths, and to compute bottom slopes and curvatures for use in wave height calculations (Munk and Arthur, 1952). Three questions arise in chosing an appropriate depth parameterization:

i) How small should the initial grid be?

ii) How should we smooth the grid points to minimize the influence of erroneous data?

iii) How sensitive will the model be to systematic errors in the depth?

Choice of a grid size will generally depend on the need to resolve significant features in the bottom topography. There appear to have been very few attempts to quantify this. Skovgaard et al. (1975) varied the grid size over a sinusoidal bar and compared the results from a computer refraction scheme with an analytic solution, but their coarsest grid spacing was only 4% of the bar wavelength, giving errors in direction of 1 degree, and in wave height of about 0.5%. Of course, a lower limit on grid size will be related to the wavelength of the waves. A fundamental assumption in the refraction equations is that the depth does not change appreciably over a wavelength, so it

should not be necessary to choose a grid size much smaller than a wavelength. In fact Skovgaard et al. (1975) apply a limiting condition which stops computation if the bottom slope becomes greater than the ratio of depth to the local wavelength.

Whether grid size is scaled to wavelength or the bottom topography, it is likely that the optimum grid size would need to be smaller in shallower water. Thus, for example, Bryant (1979) used a 200 m grid size over the continental shelf but reduced this to about 64 m in the inshore region.

It is worth noting that the criteria for choosing grid size also apply to the independence of the wave rays, and initial ray spacing is generally chosen equal to the grid spacing. Some programs (e.g. Jen, 1969) add wave rays if divergence causes the rays to become further apart than some multiple of the initial spacing (1.5 in the example cited).

Abernethy and Gilbert (1975) made a careful study of wave refraction in which they found that conventional refraction diagrams were very sensitive to frequency, offshore direction and position. This sensitivity is greatest in those regions where the refraction coefficient is large. The pairs of Figures (4.1 and 4.2) shown from their work exhibits quite strikingly the small scale variability of refraction diagrams.

In practice smoothing of the grid points is necessary to avoid unrealistic effects, particularly on the spatial derivatives of the depth, due to errors or local depth variations. Poole (1975) compared observations of wave refraction by aerial photography in Saco Bay, Maine, with three computer refraction schemes, involving quadratic least squares smoothing, cubic least squares smoothing and

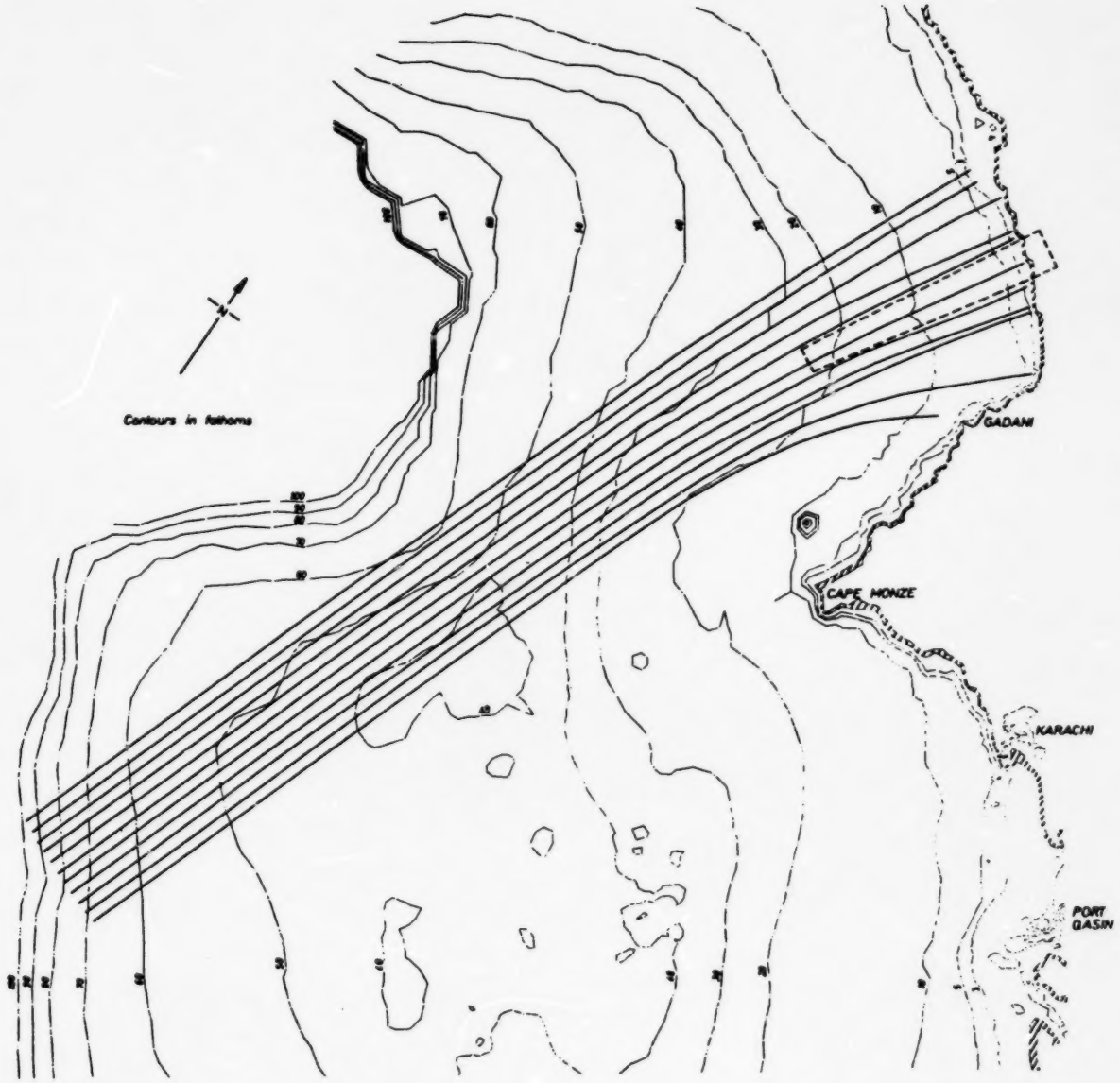

Figure 4.1 Example of a conventional refraction diagram after Abernethy and Gilbert (1975). Wave rays in the dashed portion are shown in Figure 4.2.

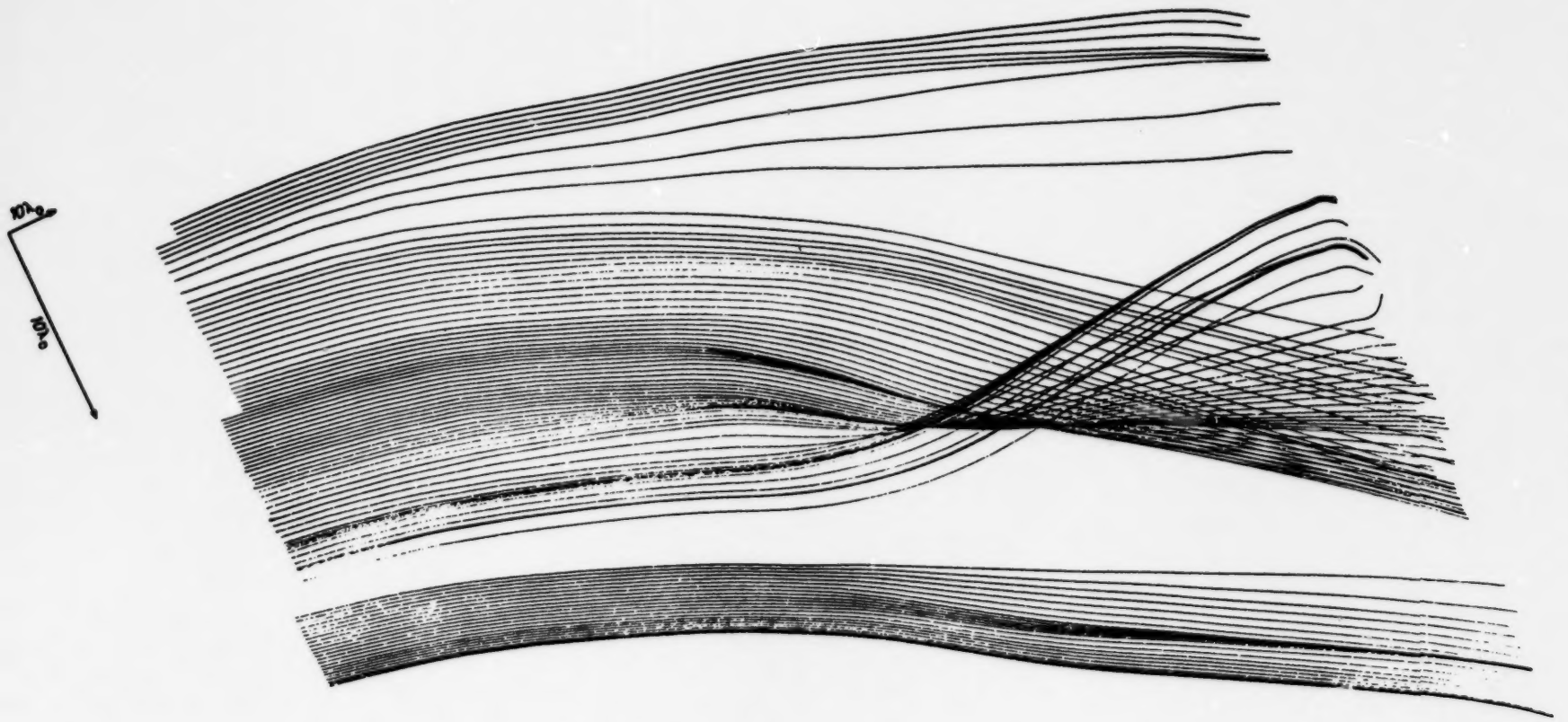

Figure 4.2 Segment of conventional refraction diagram using closely spaced rays ($0.2\lambda_o$). This diagram is expanded four times normal to the ray direction for clarity. The complete refraction diagram is shown in Figure 4.1.

constrained bicubic polynomial interpolation with no smoothing. He concluded that all techniques agreed 'equally well' with the aerial photographs, apart from one anomalous ray in the unsmoothed interpolation program, suggesting that the wave crest locations were not sensitive to the smoothing used. However the local wave height distributions varied substantially between the models. Poole concluded that further field work would be needed to determine which of the smoothing techniques worked best in practice.

Bryant (1974) looked at the sensitivity of refraction patterns to systematic errors in depth in a shallow water (depths less than 16m) refraction calculation. As expected, errors were most apparent where refraction was strongest, but Bryant concluded that the ray paths were relatively insensitive to the kind of errors which might arise from surveying errors. Clearly, however, this kind of effect is strongly dependent on the relative magnitude of the depth error and the length of the ray path, and it is therefore difficult to find general rules for assessing likely errors.

4.1.2 Treatment of Caustics

Although theoretical and laboratory studies of 'caustics' (regions where rays cross each other) are relatively advanced (e.g. Chao, 1971; Lozano and Liu, 1980), the practical handling of caustics in wave refraction programs is generally very primitive. Several approaches have been used. The most common approach seems to be to allow waves to travel through the caustics and simply recognize that calculated wave heights close to the caustics will be in error. According to Pierson (1972a) this is a reasonable approach if the areas of interest are sufficiently far from caustics and the wave does not break in the region of the caustic, since theory shows that the main far field effect on a monochromatic wave is only a phase shift. Bryant (1979) arbitrarily assigns a maximum wave height increase of 2 around a caustic, based

on laboratory and theoretical predictions. The DHI wave refraction scheme, on the other hand, stops computing wave rays which come within one wavelength of crossing (Skovgaard et al., 1975), thus admitting to ignorance about conditions near a caustic. Yet another approach, suggested by Bouws and Battjes (1982), is to assume that each ray carries with it a parcel of energy (a 'hydron'), and thus find mean energies in the grid squares based on the number of rays passing through the grid squares, regardless of whether they cross.

As discussed earlier, the continuum of frequencies present in a spectrum of waves prevents the wave amplitude becoming infinite at a caustic and this conceptually reduces the problem. The technique of Bouws and Battjes discussed above implicitly recognizes this, since decreasing the grid size around a caustic will be accompanied by an increase in the number of rays per unit crest length, each carrying less energy; in the limit that the grid becomes infinitely small, the energy carried by the rays crossing at a caustic becomes infinitely small also.

Nevertheless wave heights do increase significantly near caustics, and the effects of diffraction and wave breaking are not well handled, or understood, in practical situations. There is a clear need for more quantitative testing of the combined refraction-diffraction programs with field data. Wave breaking near caustics also needs to be further investigated by field studies. As Pierson (1972a) comments, "it seems rather simplistic to assume that some limiting height to length ratio" (or height to depth ratio) "will determine breaking, considering the very strange shape of the waves near the caustic".

4.1.3 Comparisons with Observations

There have been surprisingly few quantitative comparisons made between monochromatic wave refraction calculations and field measurements. Wavelengths and directions can be seen in aerial photographs and have therefore been compared by various authors (e.g. Poole, 1975; Bryant, 1974), but wave heights are much more difficult to compare quantitatively.

Where wave height comparison have been made agreement has been reasonable (e.g. Bryant, 1979; Aranuvachapun, 1977), but the uncertainties in the observations and predictions are very large. Figure 2.1 shows, as an example, the comparison made by Bryant (1979).

Surprisingly, there also do not seem to have been any direct comparisons between the monochromatic refraction schemes and the spectral schemes for any natural site.

In conclusion, while present wave refraction programs appear to be satisfactory in a regionally averaged sense, they are locally very unreliable, and there is insufficient field data at present to improve them. In regions with strong refraction, and especially where caustics are predicted, existing models should be used with extreme caution. The practical relevance to navigation of wave refraction, has been exemplified by Pierson (1972b), who discussed the case of the loss at sea of two British trawlers.

4.2 Applications of Shallow Water Wave Models

4.2.1 Spectral Models

The full equation for the transformation of spectral energy density $S(\underset{\sim}{k},\underset{\sim}{x})$ in the presence of a current $\underset{\sim}{U}(\underset{\sim}{x})$ and non-conservative processes $Q(\underset{\sim}{k},\underset{\sim}{x})$ [which include dissipation, generation and nonlinear transfer process] is (Phillips, 1977)

$$\left[\frac{\partial}{\partial t} + (\underset{\sim}{v} + \underset{\sim}{U})\cdot\nabla\right] S + \underset{\approx}{R}\cdot\nabla\underset{\sim}{U} = Q \qquad (4.1)$$

where $\underset{\approx}{R}$ is the radiation stress tensor (Longuet-Higgins and Stewart, 1960,1961). For the case of no currents, and Q set to zero this equation reduces to the simple form given in equation (2.5) and it is with this form that traditional spectral calculations have been made. However, there have been a number of recent numerical calculations which attempt to account for some or all of the mechanisms included in Q. These results will be discussed briefly in this section.

As noted earlier, Collins (1972) included wave generation, a simplified form of bottom friction dissipation, and an equilibrium spectrum form of wave breaking. Using the ray tracing technique he calculated spectra for linear parallel contours and for fully three-dimensional bathymetry. Typical comparisons with observations are given in Figure 4.3. Fair agreement is found (no details are given of the locations of Stages I and II). Collins remarks that the much simpler parallel bottom model appears to work as well as the three-dimensional model and suggests that two-dimensional models may be adequate in many instances.

Cavaleri and Rizzoli (1981) used very similar techniques to Collins (1972) to calculate wave spectra for the Adriatic Sea and Tyrrhenian Sea. They included wave generation, saturation and bottom friction, and for some of their results needed to include a limiting breaker height as some

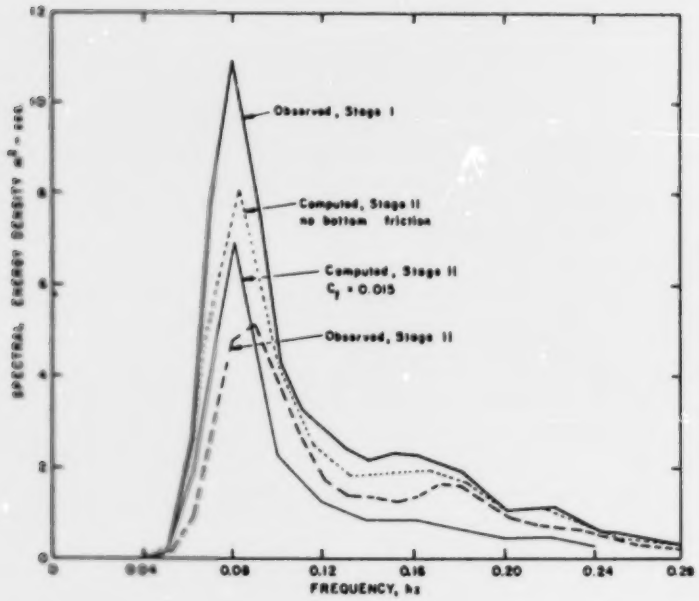

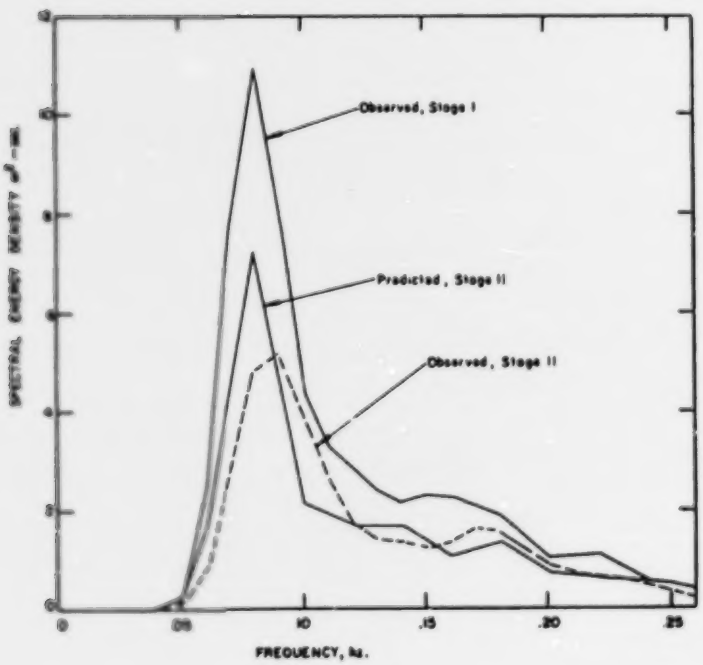

Figure 4.3 Computed and observed spectra using parallel bottom topography (top) and irregular bottom topography (bottom) from Collins (1972).

proportion of local water depth. In this case waves are entirely generated within the modelled region. Comparisons with observations are only fair (Figure 4.4). In common with Collins and others, they remark on the sensitivity of their predictions to specification of the wind field, and suggest that this is the main limitation on the accuracy of their scheme. This is of course a problem with all wave hindcasting models and has no special relevance to shallow water transformations.

Wang and Yang (1981) present calculations and data for spectral transformation within 900 m of the shore in very shallow water. No generation effects were included but bottom friction and a wave breaking criterion was used. Comparisons with field data are highly variable (Figure 4.5) and generally poor at both high and low frequencies. The inclusion of friction, using a constant friction coefficient, generally improved the comparison somewhat. The authors also show the sensitivity of the model to the assumed direction of approach of the incident waves (Figure 4.5).

Shemdin et al. (1980) present what is probably the most complete calculation of wave spectral transformation in shallow water. They include generation, bottom friction, wave-wave interactions, percolation, and wave-induced bottom motion. Comparison is made for transformation between 17 m and 13 m depth over a propagation distance of about 18 km. Examples of the comparisons are shown in Figure 4.6. It can be seen that the agreement is generally very good, except at high frequencies where the authors remark that wave-breaking, near-surface turbulence, and possibly strong interactions with long waves are not adequately modelled.

It appears from these results that there is as yet insufficient field data for an adequate test of the rather sophisticated theory that exists to describe spectral

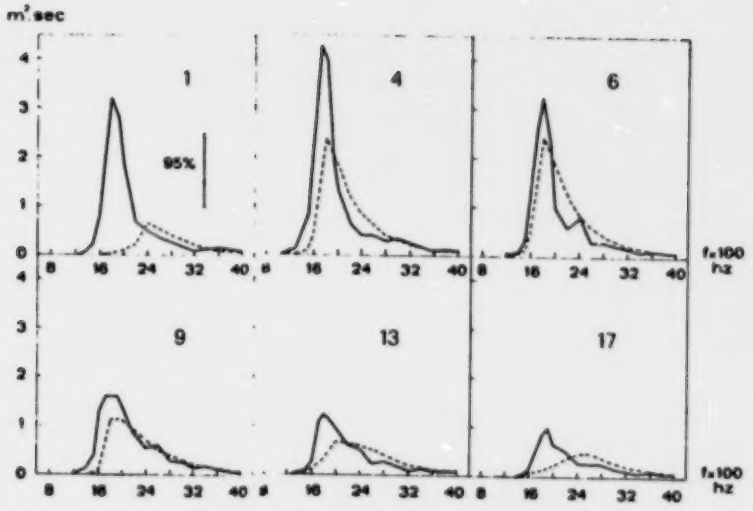

Figure 4.4 Spectra of six records during March 10, 1976, storm; 95% confidence limits are shown aside spectrum of record number 1. Dashed line shows the hindcasts of the model. From Cavaleri and Rizzoli (1981).

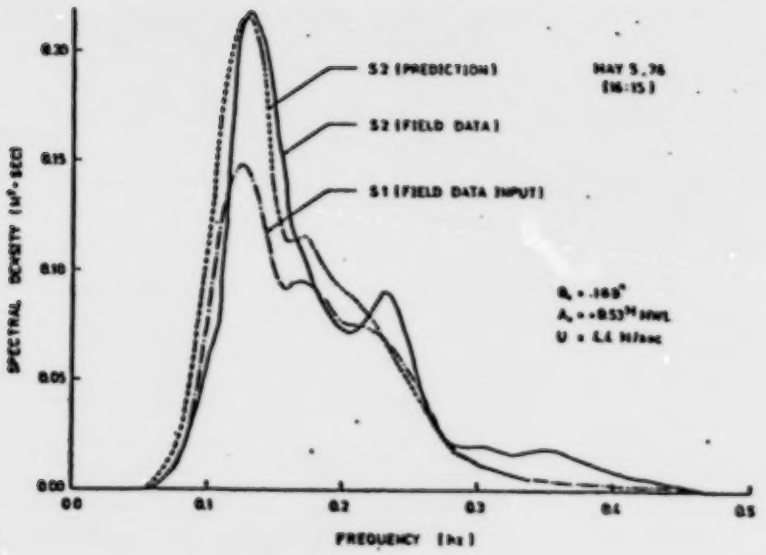

Figure 4.5a Comparison of measured and computed deep water spectral transformation (data from May 5, 1976 at 16:15, case 3). From Wang and Yang (1981).

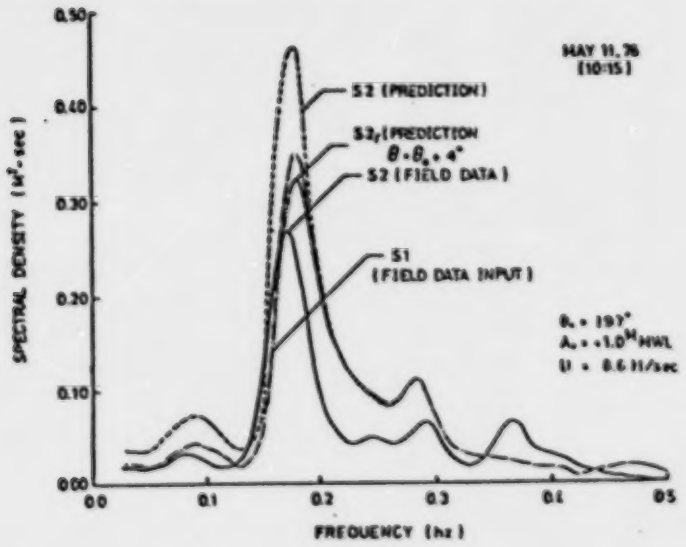

Figure 4.5b Comparison of measured and computed deep water spectral transformation (data from May 11, 1976 at 10:15, case 6). From Wang and Yang (1981).

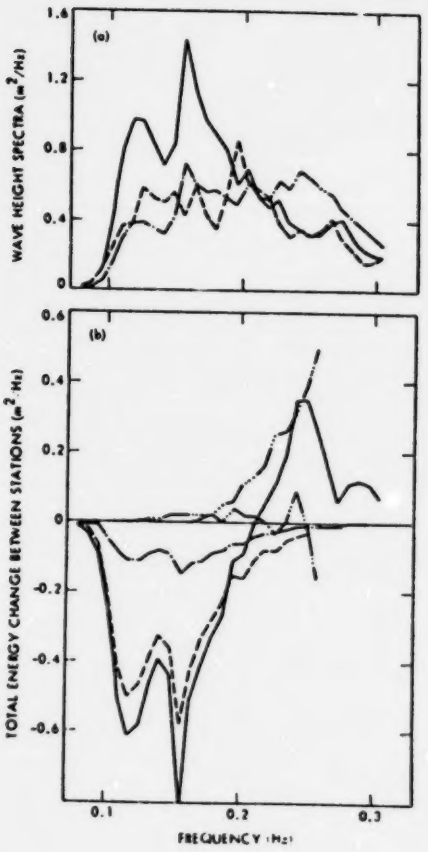

Figure 4.6 Wave transformation in finite depth water, the solid curve is the measured spectrum, dashed curve denotes the measured spectrum inshore and the dot dashed curve is the computed spectrum inshore using the solid curve as input. The energy changes computed in the lower panel include frictional dissipation (--) refraction and shoaling (-·-), nonlinear wave transfer (-···-), all adding up to the solid curve. From Shemdin et al. (1980).

transformation in shallow water. This lack of tests of the theory makes it difficult to assess the value of including the various generation, dissipation and interaction effects in operational calculations. Unfortunately a satisfactory test would require a great deal of instrumentation and may take some time to achieve. Airborne remote sensing techniques hold some promise of providing the required data (Pawka et al. 1980).

Although the addition of bottom friction, nonlinear interactions and other effects does appear to improve the predictions under certain circumstances, the improvement is only achieved at the expense of substantial computing time (as an extreme case, Freilich's (1982) calculation of wave-wave interaction took 100 hrs. of integration on a fast (Perkin-Elmer 8/32) minicomputer with highly optimized code to compute 8 spectra and associated cross-spectra). Inclusion of some of these effects will probably only be justified under circumstances where the most accurate results are required for engineering design or analysis purposes.

4.2.2 A Simplified Wave Height Model

Often the engineer needs only wave height information in shallow water and not the complete one or two-dimensional spectrum. Then a significant wave height, proportional to the area under the frequency spectrum, will suffice, and the expense of computing a spectral result by the methods described above can be avoided. Vincent (1982) has described a method for obtaining a depth-limited significant wave height, H_ℓ, based on the shallow-water spectral form described by Kitaigorodskii et al. (1975). This spectral form provides an estimate of the upper limit on energy density in water depth h as a function of frequency and wave generation as expressed in the Phillip's parameter α. Using a low-frequency cutoff value f_c, the spectrum is integrated to give the depth-limited 'significant' wave height H_ℓ,

$$H_\ell = 4 \left[\int_{f_c}^{\infty} \alpha g^2 \phi(\omega_h)/(2\pi)^4 df \right]^{\frac{1}{2}} \qquad (4.2)$$

ϕ is a function involving frequency, depth and gravity (Kitaigorodskii et al., 1975). Typical curves for H_ℓ are

shown in Figure 4.7 for three different cutoff frequencies. Use of this method requires estimates of f_c, from wave measurements in deep water, and α which can be obtained from the spectral peak frequency f_p and the wind speed U using the relationships derived by Hasselmann et al. (1973). f_p must be obtained from measurements or hindcasts.

One interesting result of this approach is that for the condition $2\pi f\sqrt{h/g} < 1$,

$$H_\ell = \frac{1}{\pi} (\alpha g h)^{\frac{1}{2}} f_c^{-1} \qquad (4.3)$$

showing that $H_\ell \propto \sqrt{h}$ when the primary spectral components are depth-limited. On the other hand, the monochromatic depth-limited wave height H_d varies linearly with h. Support for the $\sqrt{h}$ variation is shown in Figure 4.8 from measurements made by the Coastal Engineering Research Centre, U.S. Army, (CERC) (Vincent, 1982). We note that the water depths in Figure 4.8 are very shallow, ranging from 10 down to 1 m.

Because the value of H_ℓ is derived from the area under the spectrum it corresponds with the deep water definition of significant wave height, Hm_o, calculated from the variance spectrum. For most practical purposes $Hm_o \cong H_{1/3}$ in deep water; as Vincent points out, however, H_ℓ will be different from $H_{1/3}$ in shallow water but by a presently unknown amount. In conventional practice $H_{1/3}$ is usually specified in deep water and is then refracted and shoaled into shallow water until $H_{1/3} > H_d$ at which point $H_{1/3}$ is set equal to H_d. Vincent's work shows, however, that H_ℓ, which is proportional to $\sqrt{h}$, is normally much less than H_d. The spectral approach thus points to a different interpretation of the shallow water results from that usually made in coastal engineering practice. Vincent (1982) argues in favour of H_ℓ as a significant wave height appropriate in applications where the energy is of concern, and suggests that H_d be regarded as a maximum individual wave height. The relation between H_ℓ and the

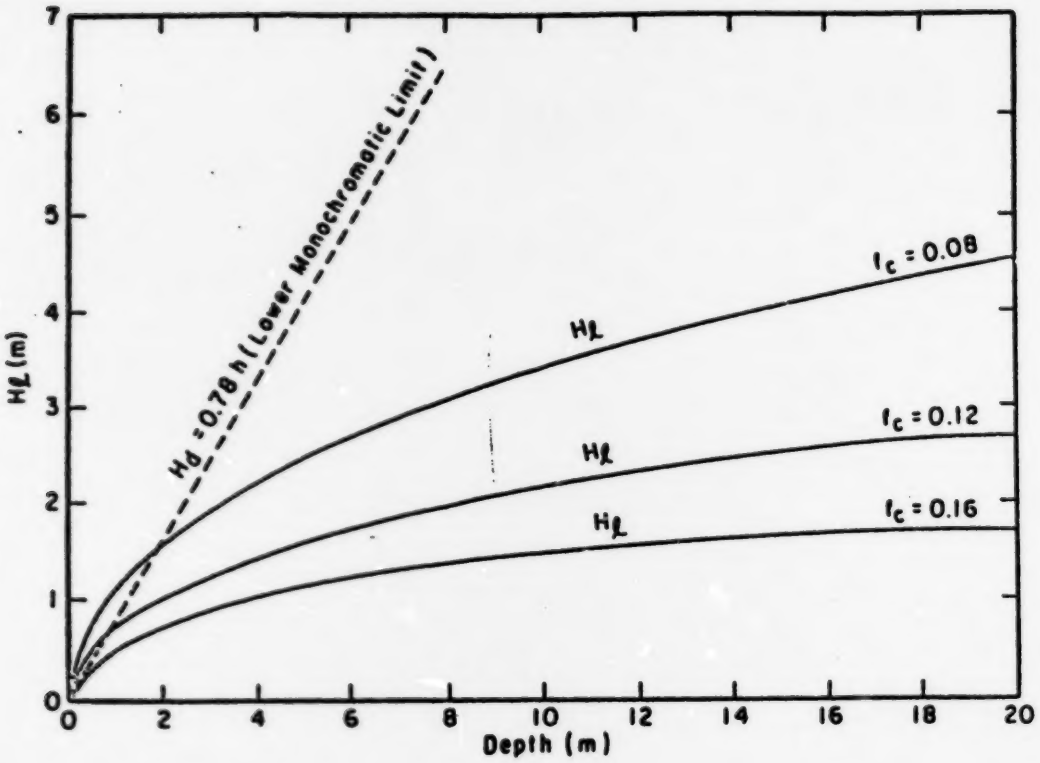

Figure 4.7 Depth-limited significant wave height, H_ℓ, as a function of water depth and cutoff frequency. Curves are calculated for $\alpha = 0.0081$. H_d is plotted for lower limit of 0.8 h. Note the critical dependence on the value assumed for f_c. From Vincent (1982).

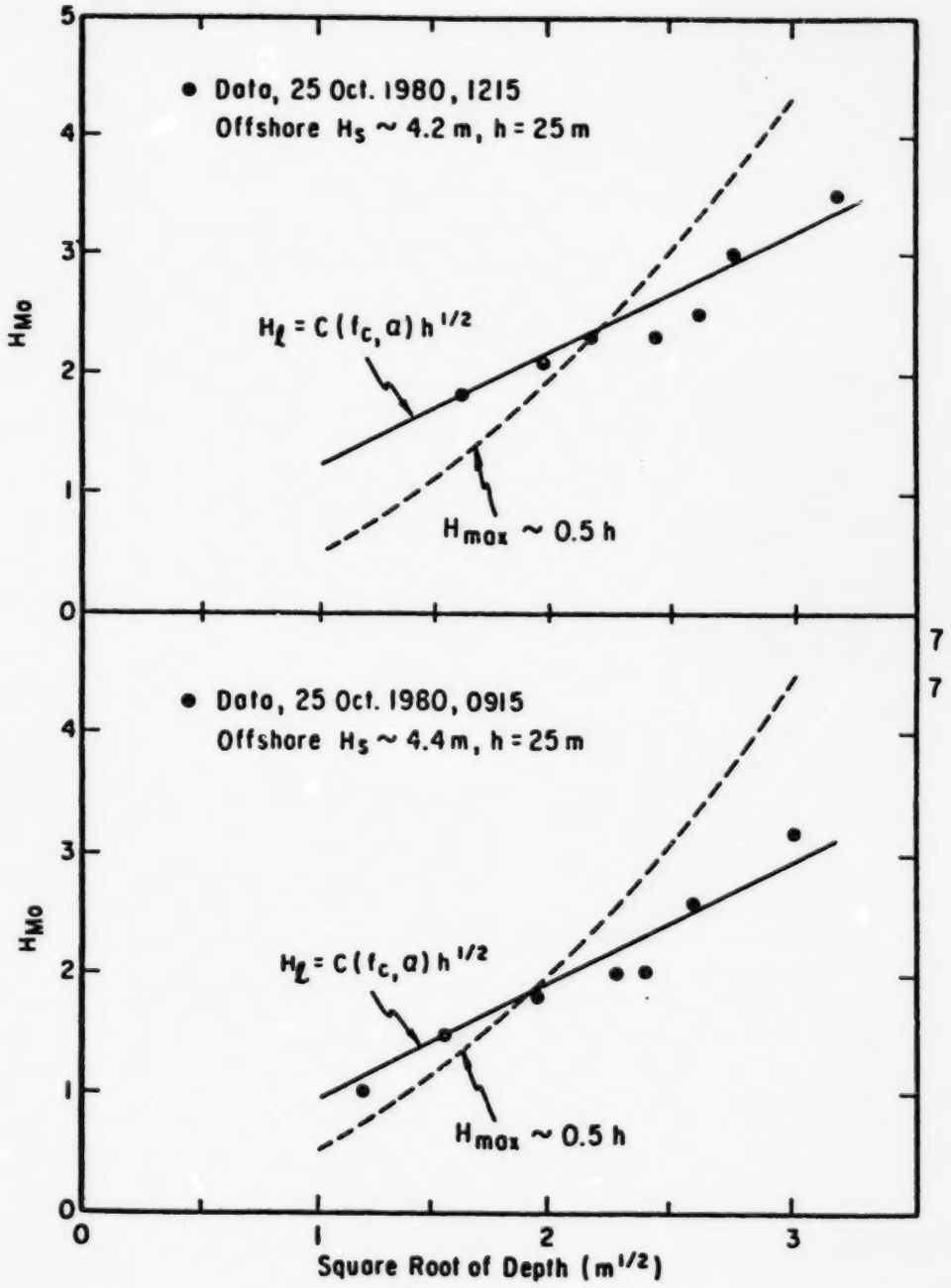
• Data, 25 Oct. 1980, 1215
Offshore $H_s \sim 4.2$ m, h = 25 m
H_{Mo}
$H_\ell = C(f_c, \alpha)\, h^{1/2}$
$H_{max} \sim 0.5\, h$
• Data, 25 Oct. 1980, 0915
Offshore $H_s \sim 4.4$ m, h = 25 m
H_{Mo}
$H_\ell = C(f_c, \alpha)\, h^{1/2}$
$H_{max} \sim 0.5\, h$
Square Root of Depth ($m^{1/2}$)

Figure 4.8 Variation of wave height with square root of depth, 25 October 1980, Duck, North Carolina. Solid line is based on measured α and f_c. Dashline represents monochromatic theory with H=0.5 h. From Vincent (1982).

spectrum area is based on a Rayleigh distribution of wave heights. In shallow water this distribution has been modified to include depth (Massel, 1978); just what effect the difference in the distribution functions for wave height would have on the interpretation of H_{ℓ} has not been reported.

4.2.3 A Non-Spectral Model

An alternative to the spectral models based on equation (4.1) is obtained by numerically integrating the Boussinesq equations for irregular wave boundary conditions. Abbott et al. (1978) have computed solutions to these equations in the form derived by Peregrine (1967) and to extensions to those equations incorporating frictional effects and porous media flows. The equations are applicable to the propagation of long waves (i.e. where the wave length is still large compared with the water depth) in arbitrary directions and having small to moderate amplitudes (Ursell number $<<O(1)$). This approach has the advantage that refraction, diffraction and reflection processes are modelled within the one scheme. Dissipation by bottom friction is included.

The high-order terms in the Boussinesq-type equations are rewritten using the linearized wave equations (see e.g. Long, 1964) to provide forms suitable for finite difference approximation. Solutions are obtained on a regular grid of points using an implicit finite-difference scheme accurate to third-order in all differentials and coefficients. The scheme evolved from the alternating direction implicit method published by Abbott et al. (1973) for the shallow-water long-wave equations (hydrostatic pressure distribution); further details are given in Abbott (1978).

Because this numerical scheme is implicit the time-step is independent of the grid size. Performance testing by Abbott et al. (1978) has shown that in many applications

run at a Courant Number[1] of approximately one, the number of points per wavelength in time and space could be reduced to as low as 6, which provides time steps of about 1 s and space increments of the order of 10 m. Cnoidal wave solutions were accurate in the sense of negligible amplitude and phase speed errors. Solutions calculated at larger Courant numbers are possible but would require greater wave resolution for accuracy so that little or nothing would be gained in computational efficiency.

Comparison of numerical results for shoaling waves with experimental data (Madsen and Mei, 1969) is shown in Figure 4.9. Here the wave crest elevations and wave heights (non-dimensionalized by the deep water amplitude η_o) are plotted for comparison purposes. The agreement between computed and observed results is quite satisfactory, particularly the departure from linear theory for relative depths less than about 0.30. In another application, Hanstholm harbour in Denmark was modelled in two-dimensions with the numerical scheme and results for the wave amplification factors derived from the mathematical model were compared with physical model results (Figure 4.10). Again, the agreement is within the experimental error of the observed data.

---

[1] The Courant Number is defined as the ratio of the integration time step Δt, to the critical time step $\Delta t_c = \Delta x/c_{\pm}$ where Δx is the spatial increment and $c_{\pm}$ are the wave celerities generated by the governing differential equations.

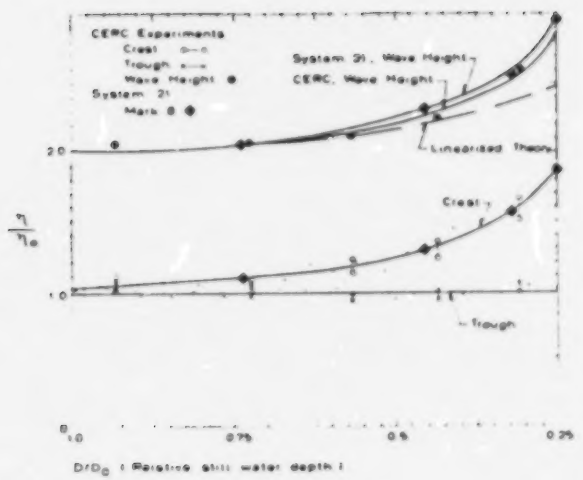

Figure 4.9 Comparison of numerical computations of shoaling waves obtained from the System 21 Mark 8 model (Abbott et al., 1978) in a one-dimensional mode, with the experimental results of Madsen and Mei (1969), labelled CERC Experiments.

IRREGULAR WAVES

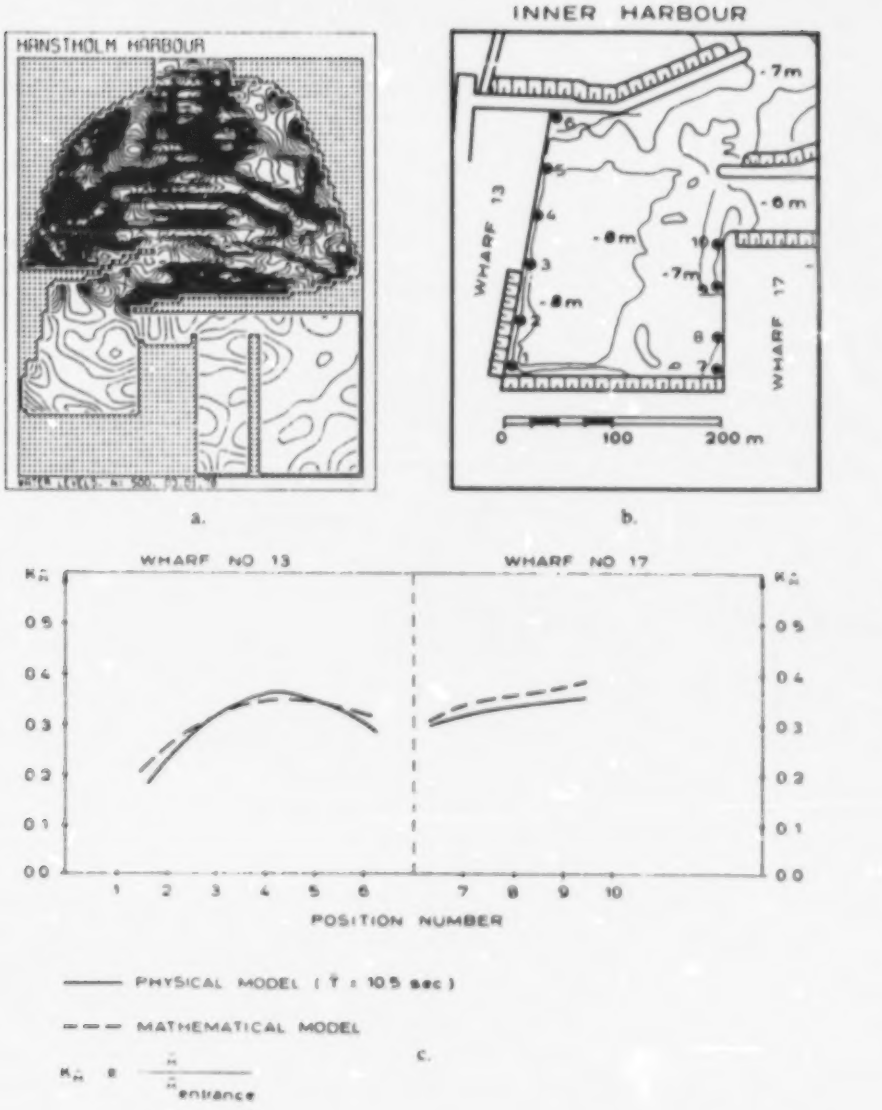

Figure 4.10 Comparison of numerical results with measurements from a physical model.

a. Surface elevation contours with irregular waves (Significant wave height ≈1.5 m).
b. Measuring stations in the physical model.
c. Comparison between amplification factors obtained in the first inner harbour in the physical model with those computed using the mathematical model, for tests with irregular, field-measured waves applied at the harbour entrance. (From Abbott et al., 1978).

5. TOWARD PRACTICAL MODELLING SYSTEMS

To conclude this review of shallow-water wave modelling we return to the problem of estimating design wave conditions for sites or areas where bathymetric effects are important and where the basic deep water wave information will be derived from meteorologically-based hindcast models. Two figures are presented (Figures 5.1a and 5.1b) to illustrate the relevance of this type of modelling: the first shows that portion of the southern Beaufort Sea where the water depths are shallow enough to refract and shoal 10 second period waves, and the second shows the analogous situation for 12 second period waves on Sable Island Bank. The majority of the proposed offshore oil and gas production facilities fall within the shaded regions. Thus accurate wave prediction in these areas must incorporate refraction and dissipation processes.

We shall consider the deep water information to be derived from conventional discrete spectral wind wave models; for a review of these models see Dexter (1974), Resio and Vincent (1979), Cardone and Ross (1979), and Earle (1981). In this class of model the wave energy density is parameterized into discrete frequencies and directions at each grid point of a regular mesh laid over the area of interest. When used for ocean-wide wave prediction the mesh must necessarily cover the whole ocean; in this way local wind-sea and swell are continuously modelled throughout the solution domain. Consequently the grid spacings used are rather coarse, of the order of 100 to 300 km, to keep computational costs within reasonable limits. For most structural design purposes the local wind-sea during severe storms is of primary concern; swell, if it is important, can be introduced as a boundary condition to the wave energy calculation so that we do not necessarily have to think in terms of meshes

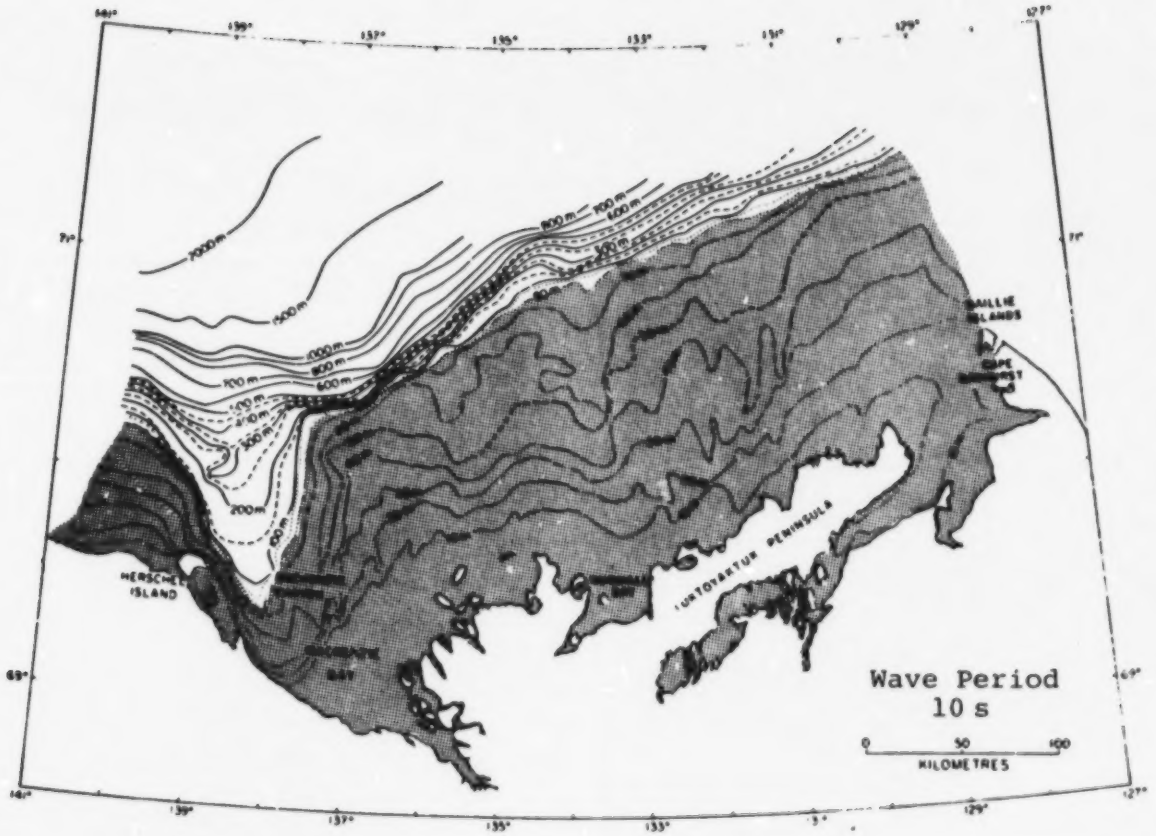

(a)

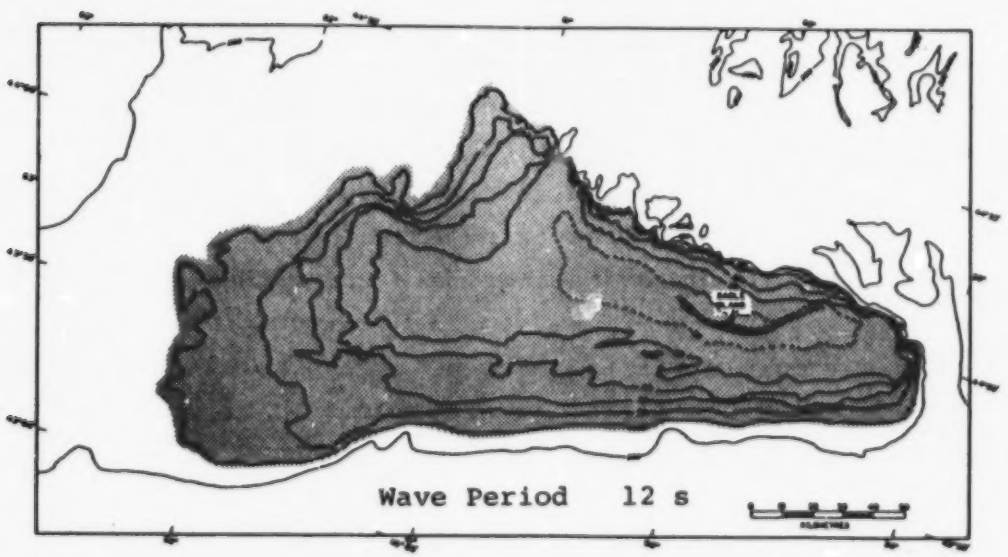

(b)

Figure 5.1 Maps of the Beaufort Sea (a) and Sable Bank (b) showing the areas where bathymetric modification of waves takes place.

covering the entire Atlantic Ocean for wave prediction on the Canadian East Coast.

Three discrete spectral models have been applied in Canadian waters and are useful for reference in the following discussion. Resio's (1981) model is presently under development by Fisheries and Oceans for applications in a hindcast mode, and the SAIL (Greenwood et al., 1982) and DHI System 20 (Hodgins, 1983; Sand et al., 1982) models have been applied by the offshore oil industry. Each model has both merits and demerits: Resio's model is based primarily on parameterizing the nonlinear wave-wave interaction process, the SAIL model incorporates a sophisticated growth formulation, also modelling the wave-wave interaction process, and the DHI System 20 model incorporates refraction into the energy propagation scheme, but neglects the wave-wave interaction mechanism in modelling spectral growth. In terms of oceanic hindcasts each model can be verified and the differences between them are not central to the discussion here. The DHI System 20 model is, however, the only one to attempt including the shallow-water effects directly into the energy conservation equation and solve for them at every time step.

5.1 Consideration of Scales, Resolution and the Consequences

To adequately hindcast deep water wave conditions the spectral model must resolve the temporal and spatial variations of the weather system, the coastlines and any islands which may produce spatial variations in the wave fields due to sheltering. Moreover, it must incorporate major bathymetric features if these modify low-frequency energy propagation. We are considering here not shoaling conditions, but refraction by the outer shelf in Mackenzie Bay, Sable Island Bank, Banquereau Bank or the Grand Banks of Newfoundland. Finally it must cover the range of wave frequencies (or wave

numbers) to be expected and resolve these adequately well to give good low-frequency detail where this is important.

To model the shallow-water transformation of wave energy the important bathymetric details must also be resolved, down to a lower limit of about one wave length. These scale and resolution requirements are summarized as order of magnitude estimates in Table 5.1. The storm system size is based on two diameters of large winter storms on the East Coast so that wave growth due to winds on the leading edge of the system is modelled, as well as growth due to winds on the trailing side, as the storm moves past the site. The resolution requirement of 50 km reflects about the largest grid spacing possible for modelling the variations in wind on either side of and along fronts embedded in these large-scale storms. Individual waves are included in Table 5.1 at the smallest scales to reflect the resolution requirements of a model that integrates Boussinesq-type equations such as described in Section 4.2.3. This order of detail would not be relevant to shallow-water spectral or wave-ray tracing calculations. Finally, frequency and direction ranges are given, together with desirable discretizations.

A complete solution to an energy conservation equation like (4.1), taking the wind field as input and predicting wave spectra in shallow water, along the shoreline of Sable Island of Mackenzie Bay for example, would require a grid large enough to model the storms with a spacing small enough to resolve the near-shore bathymetry. As an extreme example, for a uniform grid the number of mesh points would be of $O(10^9)$ (using the dimensions given in Table 5.1). If the spectrum has 30 frequencies by 24 directions, or 720 degrees of freedom, then $O(10^{12})$ spectral components would need to be computed at every time step, Δt.

Table 5.1

Scales and resolution requirements for a wave modelling system.

Physical Feature	Size (m)	Resolution (m)	Comment
storm system	3×10^6	5×10^4 [1]	cover all fetches relevant to site; must resolve weather system fronts and their motion
coastlines	1×10^5	2×10^4	delineate fetch properly and resolve coastline features
marginal sea ice zone	1×10^5	2×10^4	resolution consistent with quality of ice data available
islands	1×10^4	2×10^3	resolve features such as Sable or Herschel Island
bathymetry (detailed)	1×10^3	1×10^2	resolve bottom features important to refraction, shoaling or reflection
waves	1×10^2	10	resolution to give 10 points per wavelength
wave spectrum	Range	Resolution	Comment
frequency	0.04 to 0.33 Hz	0.010Hz [2]	gives 30 frequency bins
direction	0 to 360°	15°	gives 24 directional bins

[1] $\Delta s \sim O(10^4)$ probably required to resolve Arctic low systems in Beaufort Sea (see Hodgins, 1983), where Δs = grid spacing.

[2] Gives barely adequate resolution for periods above 16 s; non-uniform frequency discretization is desirable but yields a more complex computer code.

In storms characterized by transitory lows the rate of change in wind speed and the behaviour of the growth terms in the discrete spectral model implies a maximum time step for adequate resolution. This is usually governed by the temporal resolution of the atmospheric data available to drive the model--in most cases this is 3-hourly data at best.

A modelling consideration may, however, be more important than the wind field data in determining the time step. The spectral models use finite difference methods to solve the propagation term $(\underset{\sim}{V} + \underset{\sim}{U})\cdot\nabla S$ in (4.1) and most of these schemes are limited by the CFL linear stability condition (Richtmeyer and Morton, 1966). They require the operational Courant Number, C_r, to be less than one; this makes the choice of Δt dependent upon Δs and $|\underset{\sim}{V} + \underset{\sim}{U}|_{max}$, the combined 'group velocity' of the wave energy. The DHI System 20 uses a Lagrangian scheme which is not stability limited to $C_r \leq 1$, but from a purely programming point-of-view it is most conveniently run at this condition for the treatment of boundary data.

Thus if $C_r = (|\underset{\sim}{v} + \underset{\sim}{U}|\Delta t_{max})\Delta s = 1$,

$$\Delta t_{max} \sim \frac{\Delta s}{|\underset{\sim}{v} + \underset{\sim}{U}|} \qquad (4.2)$$

For $f = 0.04$, $\underset{\sim}{v} \cong 20$ m/s; say $\underset{\sim}{U} \sim 1$, m/s then $\Delta t_{max} \sim 0.05\Delta s$ in seconds. If the value for Δs is $O(10^2)$ m to resolve the bathymetry for refraction and shoaling conditions, then $\Delta t_{max} \sim 5$ s. For a storm lasting 36 hours to peak conditions, and allowing spin-up time for the model (matching of initial conditions to the actual wind field), this time step gives about 3×10^4 solution steps. Combining this with the number of spectral components per time step derived above

yields $O(10^{16})$ solution values for the storm. Typical computer times are $O(10^{-4})$ CPU seconds per value (DHI System 20 model including refraction) which gives a run time of $O(10^{12})$ seconds, or 30,000 years. One would be far better off to measure the required wave data!

Although an extreme example, this argument shows why spectral models are run with spatial increments of 50 to 300 km, and also why considerable effort is devoted to reducing the number of degrees of freedom in the spectra, particularly for high frequencies which are usually saturated in storm conditions. It also points out very clearly the need for nested grids with increased resolution only in those areas which require definition of islands or important bottom features, and the use of an efficient refraction calculation to provide wave spectral data in shallow water. A recommended modelling strategy is discussed in the next section, together with data requirements for developing and verifying these models.

5.2 A Recommended Strategy

To date the deep water wind-wave models applied on the East Coast have not attempted to incorporate Sable Island into the grid and model its influence on the wave field over Sable Bank. This would be an important step, however, for providing accurate boundary data to any subsequent calculation of refraction and shoaling. The situation in the Beaufort Sea is slightly different in that the major concern of the deepwater model is to provide accurate boundary data incorporating the influence of moderate refraction by the continental shelf, as close as possible to the shoreline. In this way the areal coverage required in a shallow water refraction and shoaling model is minimized for any given near-shore site. This was attempted using a 40x40 km grid in a hindcast study of the area with the DHI

System 20 model (Hodgins, 1983) but this grid spacing is still too coarse to give good resolution of the bathymetry in Mackenzie Bay.

Thus we recommend the development of automatic change of scale capabilities within one or more existing deep water wind-wave models. This would be done by dividing the base grid, with a spacing of say 45 to 50 km, into a nested grid with spacings of perhaps 10 to 15 km, over an appropriate subregion of the modelled area. The wave growth, decay and propagation calculations would proceed from the coarse grid to the fine grid, and vice versa, within one execution step so that there would be no loss or distortion of propagating wave energy between the grids. Because of the CFL stability condition noted above, the propagation schemes used in some of the wind-wave models would need modification, essentially to schemes where the time and space steps are independent. The deep-water model must also include depth and current refraction in areas where these are important.

To obtain wave spectra at shallow-water locations with depths ranging from about three to thirty metres we recommend the development of a spectral refraction model based on reverse ray tracing into deeper water. This model would provide a directional energy frequency spectrum at the site after refraction, shoaling, dissipation, and possibly growth effects. The refraction and shoaling aspects would follow the approach used for example by Abernethy and Gilbert (1975). However, the method of including dissipation terms requires careful study, in particular for parameterizing bottom friction for a range of frequencies and other mechanisms such as percolation, bottom motion, and reflection that may be important in certain areas.

While this type of shallow-water model would not reproduce all the nuances of spectral transformation, such as finite amplitude effects leading to wave splitting or harmonics of the peak frequency, it would provide a practical modelling approach giving useful wave data. Moreover the required boundary conditions are directly available from the deep water models discussed above.

As we have noted earlier there is very little quantitative comparison between model results and shallow water wave height or spectral data. Model developments such as recommended here should logically be accompanied by measurement programs for two reasons. First the data are needed to calibrate empirical coefficients in the dissipation, and possibly growth terms. Second, data are required to validate the model results and to assess how important finite amplitude and current effects are for given areas. Because the primary output of the model is a directional spectrum, we recommend that field programs be designed to measure this type of spectrum both in deep and shallow water. In this way detailed spectral verifications can be made in addition to comparisons of such integral measures as mean wave direction, wave period or significant wave height.

6. REFERENCES

Abbott, M.B., A. Damsgaard and G.S. Rodenhuis, 1973. "System 21, Jupiter (A Design System for Two-Dimensional Nearly Horizontal Flows". J. Hyd. Res., 11(1), 1-28.

Abbott, M.B., 1978. Computational Hydraulics: Elements of the Theory of Free Surface Flows. Pitman, London.

Abbott, M.B., H.M. Petersen and O. Skovgaard, 1978. "On the Numerical Modelling of Short Waves in Shallow Water". J. Hyd. Res., 16(3), 173-204.

Abernethy, C.L. and G. Gilbert, 1975. "Refraction of Wave Spectra". Report No. INT 117, Hydraulics Research Station, Wallingford, U.K.

Aranuvachapun, S., 1977. "Wave Refraction in the Southern North Sea". Ocean Engng., 4, 91-99.

Baird, W.F. and C.W. Glodowski, 1977. "Port Elgin Harbour. Investigation of Wave Agitation and Breakwater Protection for a Marina Operation". Public Works Canada, Marine Directorate, Ottawa.

Bea, R.G., 1974. "Gulf of Mexico Hurricane Wave Heights". Proc. 6th Offshore Tech. Conf., OTC 2110, Dallas, 791-810.

Benjamin, T.B., 1974. "Lecturers on Nonlinear Wave Motion, in Nonlinear Wave Motion". Lectures in Applied Mathematics, (A.C. Newell, ed.), Vol 15, American Mathematical Society, Providence, R.I.

Berkhoff, J.C.W., 1973. "Computation of Combined Refraction-Diffraction". Proc. 13th Coastal Engng. Conf., July 1972, Vancouver (New York, A.S.C.E., 1, 471-490).

Berkhoff, J.C.W., 1975. "Linear Wave Propagation Problems and the Finite Element Method in Finite Elements". Fluids. (R.H. Gallagher, J.T. Oden, C. Taylor and O.C. Zienkiewicz, eds.), London, Wiley, Vol. 1, 251-264.

Boussinesq, J., 1872. "Theorie des Ondes et des Remous qui se Propagent le Long d'un Canal Rectangulaire Horizontal, en Communiquant au Liquide Contenu dans ce Canal des Vitesses Sensiblement Pareilles de la Surface au Fond". J. Math. Pures et Appl., 2nd Series, 17, 55-108.

Boussinesq, J., 1877. "Essai sur la Theorie des Eaux Courantes". Institut de France, Academie des Sciences. Memoires Presentes par Divers Savants, 23(1).

Bouws, E. and J.A. Battjes, 1982. "A Monte Carlo Approach to the Computation of Refraction of Water Waves". J. Geophys. Res., 87, C8, 5718-5722.

Bowen, A.J., D.L. Inman and V.P. Simmons, 1968. "Wave 'Set-Down' and 'Set-Up'." J. Geophys. Res., 73(8), 2569-2577.

Bremner, J.M., 1970. "The Geology of Wreck Bay, Vancouver Island". M.Sc. Thesis, University of B.C.

Bretschneider, C.L. and R.U. Reid, 1954. "Changes in Wave Height Due to Friction, Percolation and Refraction". Tech. Memo., Beach Environment Board, U.S. Army Corps of Engineers, No. 45.

Bryant, E.A., 1974. "A Comparison of Air Photographs and Computer Simulated Wave Refraction Patterns in the Nearshore Area, Richibucto, Canada and Jervis Bay, Australia". Maritime Sediments, 10(3), 85-95.

Bryant, E., 1979. "Comparison of Computed and Observed Breaker Wave Heights". Coastal Engng., 3, 39-50.

Cardone, V.J. and D.B. Ross, 1979. "State-of-the-Art Wave Prediction Methods and Data Requirements". Ocean Wave Climate. (Earle and Malahoff, eds.), Plenum, 61-91.

Carpenter, S.H., L.J. Thompson and W.R. Bryant, 1973. "Viscoelastic Properties of Marine Sediments". Proc. 5th Offshore Tech. Conf., OTC 1903, Dallas, 777-788.

Cavaleri, L. and P.M. Rizzoli, 1981. "Wind Wave Prediction in Shallow Water: Theory and Applications". J. Geophy. Res., 86, 10961-10973.

Chao, Y-Y, 1971. "An Asymptotic Evaluation of the Gravity Wave Field Near a Smooth Caustic". J. Geophys. Res., 79.

Chen, H.S. and C.C. Mei, 1974. "Oscillations and Wave Forces in an Offshore Harbour: Applications of Hybrid Finite Element Method to Water-Wave Scattering". Ralph M. Parsons Laboratory for Water Resources and Hydrodynamics, M.I.T. Rept. No. 190.

Collins, J.I., 1972. "Prediction of Shallow-Water Spectra". J. Geophys. Res., 77, 2693-2707.

Dalrymple, R.A. and P.L.-F. Liu, 1978. "Waves Over Soft Muds: A Two-Layer Fluid Model". J. Phys. Oceanogr., 8, 1121-1131.

Dexter, P.E., 1974. "Tests of Some Programmed Numerical Wave Forecast Models". J. Phys. Oceanogr., 4, 635-644.

Dingler, J.R., 1975. "Wave-Formed Ripples in Nearshore Sands". Ph.D. Dissertation, U. Calif., San Diego.

Dorrestein, R., 1960. "Simplified Method for Determining Refraction Coefficients for Sea Waves". J. Geophys. Res., 65, 637-642.

Dreyer, A.A., 1973. "Study of Wind-Generated Seawaves in Shallow Sea". Thesis, Inst. Oceanology, Acad. Sci. USSR.

Earle, M.D., 1981. "Problems in Ocean Wave Hindcasting". Spaceborne Synthetic Aperture Radar for Oceanography (Beal et al., eds.), Johns Hopkins Univ. Press, Baltimore, 98-109.

Freilich, M.H., 1982. "Resonance Effects on Shoaling Surface Gravity Waves". Ph.D. Thesis, University of California, San Diego, Scripps Institute of Oceanography.

Gade, K.G., 1958. "Effects of a Nonrigid, Impermeable Bottom on Plane Surface Waves in Shallow Water". J. Marine Res., 16, 61-82.

Gallagher, B., 1972. "Some Qualitative Aspects of Non-Linear Wave Radiation in a Surf Zone". Geophys. Fluid Dyn., 3, 347-354.

Greenwood, J.A., V.J. Cardone and L.M. Lawson, 1982. "Intercomparison Test Version of the SAIL Wave Model". Proc. Symp. Wave Dynamics and Radio Probing of Ocean Surface, Miami, 1981.

Griswold, G.M., 1962. "Numerical Calculation of Wave Refraction". J. Geophys. Res., 68(6), 1715-1723.

Guza, R.T. and E.B. Thornton, 1980. "Local and Shoaled Comparisons of Sea Surface Elevations, Pressures and Velocities". J. Geophys. Res., 85, 1524-1530.

Hamilton, E.L., 1979. "Vp/Vs and Poisson's Ratios in Marine Sediments and Rocks". J. Acoust. Soc. Amer., 66, 1093-

Hasselmann, K. and J.I. Collins, 1968. "Spectral Dissipation of Finite-Depth Gravity Waves Due to Turbulent Bottom Friction". J. Marine Research, 26, 1-12.

Hasselmann, K., T.P. Barnett, E. Bouws, H. Carlson, D.E. Cartwright, K. Enke, J.A. Ewing, H. Gienapp, D.E. Hasselmann, P. Kruseman, A. Meerburg, P. Müller, D.J. Olbers, K. Richter, W. Sell, and H. Walden, 1973. "Measurements of Wind-Wave Growth and Swell Decay During the Joint North Sea Wave Project (JONSWAP)". Deutschen Hydrographischen Zeitschrift, Reihe A, Nr. 12.

Hasselmann, K., 1974. "On the Spectral Dissipation of Ocean Waves Due to White-Capping". Boundary Layer Meteorol., 6, 107.

Hasselmann, K., D.B. Ross, P. Müller and W. Sell, 1976. "A Parametric Wave Prediction Model". J. Phys. Oceanogr., 6, 200-228.

Hasselmann, S. and K. Hasselmann, 1980. "A Symmetrical Method of Computing the Nonlinear Transfer in a Gravity Wave Spectrum". Report, Max-Planck-Inst. für Meteorol., Hamburg, Germany, 1980.

Hayes, J.G., 1980. "Ocean Current Wave Interaction Study". J. Geophys. Res., 85, 5025-5031.

Hodgins, D.O., 1983. "A Review of Extreme Wave Conditions in the Beaufort Sea". Report Prepared for Fisheries and Oceans, Canada, by Seaconsult Marine Research Ltd.

Hsiao, S.V. and O.H. Shemdin, 1978. "Bottom Dissipation in Finite-Depth Water Waves". Proc. 16th Internat. Conference on Coastal Engineering, Hamburg.

Hsiao, S.V. and O.H. Shemdin, 1980. "Interaction of Ocean Waves With a Soft Bottom". J. Phys. Oceanogr., 10, 605-610.

Hunt, J.N., 1959. "On the Damping of Gravity Waves Propagated Over a Permeable Surface". J. Geophys. Res., 64, 437-442.

Ijima, T., T. Matsuo and K. Koga, 1970. "Equilibrium Range Spectra in Shoaling Water". Proc. 12th Coastal Eng. Conference, Sept. 13-18, 1970, Washington, D.C., Vol. 1, A.S.C.E., 137-149.

Isaacson, M. de St. Q., 1977. "Second Approximation to Gravity Wave Attenuation". J. Waterways, Harbours, Coastal Div., A.S.C.E., 103, (WW1), 43-55.

Iwagaki, Y. and T. Kakinuma, 1963. "On the Bottom Friction Factor of the Akita Coast". Coastal Engineering in Japan, 6, 83-91.

Iwagaki, Y., Y. Tsuchiya and M. Sakai, 1965. "Bank Studies on the Wave Damping Due to Bottom Friction". Coastal Engineering in Japan, 8, 37-49.

Jen, Y., 1969. "Wave Refraction Near San Pedro Bay, California". J. Waterways, Harbours, Coastal Div., A.S.C.E., 95, 379-393.

Johnson, J.W., 1947. "The Refraction of Surface Waves by Currents". Trans. Am. Geophys. Un., 28, 867-874,

Jonsson, I.G., 1966. "Wave Boundary Layers". Proc. 10th Conference Coastal Engineering, Tokyo, A.S.C.E., 127-148.

Jonsson, I.G., O. Skovgaard and O. Brink-Kjaer, 1976. "Diffraction and Refraction Calculations for Waves Incident on an Island". J. Mar. Res., 34, 469-496.

Jonsson, I.G. and N.A. Carlsen, 1976. "Experimental and Theoretical Investigations in an Oscillatory Turbulent Boundary Layer". J. Hydraulic Research, 14, 45-60.

Jonsson, I.G. and J.D. Wang, 1980. "Current-Depth Refraction of Water Waves". Ocean Engng., 7, 153-171.

Kitaigorodskii, S.A., V.P. Krasitskii and M.M. Zaslavskii, 1975. "On Phillips' Theory of Equilibrium Range in the Spectra of Wind-Generated Gravity Waves". J. Phys. Geophys., 5, 410-420.

Kamphuis, J.W., 1975. "Friction Factor Under Oscillatory Waves". J. Waterways, Harbours, Coastal Div., A.S.C.E., 101 (WW2), 135-144.

Kamphuis, J.W., 1978. "Attenuation of Gravity Waves by Bottom Friction". Coastal Engineering, 2, 111-118.

Karlsson, T., 1969. "Refraction of Continuous Ocean Wave Spectra". J. Waterways, Harbours, Coastal Engng. Div., A.S.C.E., 95 (WW4), 437-448.

Krasitskii, V.P., 1974. "Toward a Theory of Transformation of the Spectrum on Refraction of Wind Waves". Izv. Akad. Nauk. SSSR, Atmosph. and Ocean Physics, 10, 39-44.

Krasitskii, V.P., 1974. "Toward a Theory of Transformation of the Spectrum on Refraction of Wind Waves". Izv. Akad. Nauk. SSSR, Atmosph. Oceanic Physics, 10, 72-82.

Lau, J. and A. Barcilon, 1972. "Harmonic Generation of Shallow Water Waves Over Topography". J. Phys. Ocean, 2, 405-410.

Lau, J. and B. Travis, 1973. "Slowly Varying Stokes Waves and Submarine Longshore Bars". J. Geophys. Res., 78(21) 4489-4497.

LeMéhauté, B. and J.D. Wang, 1982. "Wave Spectrum Ranges on Sloped Beach". J. Waterways, Harbours, Coastal and Ocean Div., A.S.C.E., 108, (WW1), 33-47.

Liu, P.L.-F., 1973. "Damping of Water Waves Over Porous Bed". J. Hydraulic Division, A.S.C.E., 99, 2263-2271.

Long, R.R., 1964. "The Initial Value Problem for Long Waves of Finite Amplitude". J. Fluid Mech., 20(1), 161-170.

Long, R.B., 1973. "Scattering of Surface Waves by an Irregular Bottom". J. Geophys. Res., 78, 7861-7870.

Longuet-Higgins, M.S., 1956. "The Refraction of Sea Waves in Shallow Water". J. Fluid Mech., 1, 163-176.

Longuet-Higgins, M.S., 1957. "On the Transformation of a Continuous Spectrum by Refraction". Proc. Camb. Phil. Soc., 53, 226-229.

Longuet-Higgins, M.S. and R.W. Stewart, 1960. "Changes in the Form of Short Gravity Waves on Long Waves and Tidal Currents". J. Fluid Mech., 8, 565-583.

Longuet-Higgins, M.S. and R.W. Stewart, 1961. "The Changes in the Amplitude of Short Gravity Waves on Steady Non-Uniform Currents". J. Fluid Mech., 10, 529-549.

Lozano, C. and P.L.-F. Liu, 1980. "Refraction-Diffraction Model for Linear Surface Water Waves". J. Fluid Mech., 101, 705-720.

MacPherson, H. and P.G. Kurup, 1981. "Wave Damping at the Kerala Mudbanks (SW India)". Indian J. Marine Science, 10, 154-160.

Madsen, O.S. and C.C. Mei, 1969. "The Transformation of a Solitary Wave Over an Uneven Bottom". J. Fluid Mech., 39(4), 781-797.

Madsen, O.S., 1978. "Wave-Induced Pore Pressures and Effective Stresses in a Porous Bed". Geotechnique, 28, 377-393.

Mallard, W.W. and R.A. Dalrymple, 1977. "Water Waves Propagating Over a Deformable Bottom". Proc. 9th Offshore Tech. Conf., Houston, OTC 2895.

Massel, S.R., 1978. "Needs for Oceanographic Data to Determine Loads on Coastal and Offshore Structures". IEEE J. Oceanic Engng., OE-3(4), 137-145.

Meyer, R.E., 1979. "Theory of Water-Wave Refraction". Adv. in Applied Mechanics, 19, 53-141.

Miche, R., 1944. "Undulatory Movements of the Sea in Constant and Decreasing Depth". Ann. Ports et Chaussées, 25-78; 131-164; 270-292; 369-406.

Miles, J.W., 1957. "On the Generation of Surface Waves by Stream Flows". J. Fluid Mech., 3, 186.

Munk, W.H. and R.S. Arthur, 1952. "Wave Intensity Along a Refracted Ray". Natl. Bur. Stand. Circ., 521, 95-108.

Nielsen, P., 1977. "A Note on Wave Ripple Geometry". Prog. Rep. Inst. Hydrodyn. & Hydraulic Engng., Tech. Univ. Denmark, 43, 17-22.

Noda, E.V. et al., 1974. "Nearshore Circulations Under Sea Breeze Conditions and Wave-Current Interactions in the Surf Zone". Tetra Tech., Report TC-149-4.

Pawka, S.S., S.V. Hsiao, O.H. Shendin and D.L. Inman, 1980. "Comparisons Between Wave Directional Spectra from SAR and Pressure Sensor Arrays". J. Geophys. Res., 85, 4987-4995.

Peregrine, D.H., 1967. "Long Waves on a Beach". J. Fluid Mech., 27(4), 715-827.

Petersen, M.H., 1977. "Refraction of Cnoidal Waves". Coastal Engineering, 1, 43-61.

Phillips, O.M., 1957. "On the Generation of Waves by Turbulent Wind". J. Fluid Mech., 2, 417.

Phillips, O.M., 1958. "The Equilibrium Range in the Spectrum of Wind-Generated Waves". J. Fluid Mech., 4, 426-434.

Phillips, O.M., 1977. Dynamics of the Upper Ocean. 2nd Edition. Cambridge U. Press, London.

Pierson, W.J., Jr., J.J. Tutteu, and J.A. Woolley, 1953. "The Theory of the Refraction of a Short-Crested Gaussian Sea Surface With Application to the Northern New Jersey Coast". Proc. 3rd Coastal Engng. Conf.,(J.W. Johnson, Ed.), 86-108.

Pierson, W.J., Jr., G. Neumann and R.W. James, 1955. Practical Methods for Observing and Forecasting Ocean Waves by Means of Wave Spectra and Statistics. U.S. Navy Hydrographic Office Publication No. 603.

Pierson, W.J., 1972a. "Wave Behaviour Near Caustics in Models and in Nature". Waves on Beaches and Resulting Sediment Transport. (R.E. Meyer, Ed.), Academic Press, N.Y.

Pierson, W.J., 1972b. "The Loss of Two British Trawlers - A Study in Wave Refraction". J. Navigation, 25(3), 291-304.

Poole, L.R., 1975. "Companion of Techniques for Approximating Ocean Bottom Topography in a Wave-Refraction Computer Model". Scientific & Tech. Aerospace Rpts., 14(2), 219. NASA, Langley Research Centre, Va. [NTIS N76-11677/1G1].

Putnam, J.A., 1949. "Loss of Wave Energy Due to Percolations in a Permeable Sea Bottom". Trans. Amer. Geophys. Union, 30, 349-356.

Putnam, J.A. and J.W. Johnson, 1949. "The Dissipation of Wave Energy by Bottom Friction". Trans. Amer. Geophys. Union, 30, 67-74.

Resio, D.T. and C.L. Vincent, 1979. "A Comparison of Various Numerical Wave Prediction Techniques". Proc. Offshore Tech. Conf., OTC 3642, 2471-2478.

Resio, D.T., 1981. "The Estimation of Wind-Wave Generation in a Discrete Spectral Model". J. Phys. Oceanog., 11, 510-525.

Richter, K., B. Schmalfeldt and J. Siebert, 1976. "Bottom Irregularities in the North Sea". Deutsche Hydrog. Z., 29, 1-10.

Richtmeyer, R. and K. Morton, 1966. Difference Methods for Initial-Value Problems. 2nd Edition, Interscience, New York.

Rosenthal, W., 1978. "Energy Exchange Between Surface Waves and Motion of Sediment". J. Geophys. Res., 83, C4, 1980-1982.

Ryrie, S. and D.H. Peregrine, 1982. "Refraction of Finite-Amplitude Water Waves Obliquely Incident on a Uniform Beach". J. Fluid Mech., 115, 91-104.

Sand, S.E., O. Brink-Kjaer and J.B. Neilsen, 1982. "Directional Wave Models as a Design Basis". Proc. Conf. Wind and Wave Directionality, Paris, 1981.

Sawaragi, T., K. Iwata and M. Kubo, 1976. "Consideration of Friction Coefficient for Sea Bottom". Proc. 15th Coastal Engineering Conference, Honolulu, 595-606.

Sawaragi, T. and K. Iwata, 1980. "Wave Power Spectrum Slope on High Frequency Range in Shallow Water Surf". Coastal Engineering in Japan, 23, 91-99.

Shemdin, O., K. Hasselmann, S.V. Hsiao and K. Herterich, 1977. "Nonlinear and Linear Bottom Interaction Effects in Shallow Water". Turbulent Fluxes Through the Sea Surface, Wave Dynamics and Prediction. (A. Favre and K. Hasselmann, Eds.), Plenum Press, N.Y., 347-372.

Shemdin, O.H., W.E. Brown, Jr., F.G. Staudhammer, P. Shuchman, R. Rawson, J. Zelenka, D.B. Ross, W. McLeish and R.A. Berles, 1978. "Comparison of In Situ and Remotely Sensed Ocean Waves off Marineland, Florida". Boundary-Layer Meteorology, 13, 193-202.

Shemdin, O.H., S.V. Hsiao, H.E. Carlson, K. Hasselmann and K. Shulze, 1980. "Mechanisms of Wave Transformation in Finite-Depth Water". J. Geophys. Res., 85, C9, 5012-5018.

Shiau, J.C. and H. Wang., 1977. "Wave-Energy Transformation Over Irregular Bottom". J. Waterways, Ports, Coastal and Ocean Division, A.S.C.E., 103 (WW1), 57-63.

Skovgaard, O., I.G., Jonsson and J.A. Bertelsen, 1975. "Computation of Wave Heights Due to Refraction and Friction". J. Waterways, Harb. Div. Am. Soc. Civ. Engrs, 101, 15-32.

Skovgaard, O., I.G. Jonsson and J.A. Bertelsen, 1976. "Closure to "Computation of Wave Heights Due to Refraction and Friction". J. Waterways Harb. Div. Am. Soc. Civ. Engrs., 102, 100-105.

Skovgaard, O. and I.G. Jonsson, 1977. "Current Depth Refraction Using Finite Elements". Proc. 15th Coastal Engng. Conf., Honolulu, July 1976, Chap. 41, A.S.C.E., New York, 1, 721-737.

Smith, R., 1976. "Giant Waves". J. Fluid Mech., 77, 417-431.

Tayfun, M.A., R.A. Dalrymple and C.Y. Yang, 1976. "Random Wave-Current Interactions in Water of Varying Depth". Ocean Engng., 3, 403-420.

Thornton, E.B., 1976. "Kinematics of Breaking Waves". Proc. 15th Conference Coastal Engng., A.S.C.E.

Thornton, E.B., 1977. "Rederivation of the Saturation Range in the Frequency Spectrum of Wind-Generated Waves". J. Phys. Oceanogr., 7, 137-140.

Tubman, M.W. and J.N. Suhayda, 1976. "Wave Action and Bottom Movements in Fine Sediments". Proc. 15th Coastal Engineering Conference, A.S.C.E., Honolulu, 1168-1183.

Turnstall, E.B. and D.L. Inman, 1975. "Vortex Generation by Oscillatory Flow Over Rippled Surfaces". J. Geophys. Res., 80, 3475-3484.

Van Ieperen, M.P., 1975. "The Bottom Friction of the Sea-bed off Melkbosstrand, South Africa". Deutsche Hydrog. Z., 28, 72-88.

Vincent, C.L., 1982. "Depth-Limited Significant Wave Height: A Spectral Approach". Technical Report No. 82-3, Coastal Engineering Research Centre, U.S. Army Corps of Engineers, Fort Belvoir, Va.

Vincent, C.L., W.G. Grosskopf and J.M. McTamany, 1982. "Transformation of Storm Wave Spectra in Shallow Water Observed During the ARSLOE Storm". Oceans 82 Conference, Washington, D.C., Sept. 20-22, 1982, 920-925.

Wang, H. and W.-C. Yang, 1981. "Wave Spectral Transformation Measurements at Sylt, North Sea". Coastal Engineering, 5, 1-34.

Willebrand, J., 1975. "Energy Transport in a Non-Linear and Unhomogeneous Random Gravity Wave Field". J. Fluid Mech., 70(1), 113-126.

Wilson, W.S., 1966. "A Method for Calculating and Plotting Surface Wave Rays". U.S. Army Coastal Engineering Research Centre, Technical Memo No. 17.

Yamamoto, T., H.L. Koning, H. Sellmeijer and E. Van Hijum, 1978. "On the Response of a Poro-Elastic Bed to Water Waves". J. Fluid Mech., 87, 193-206.

Yamamoto, T., 1982. "Non-linear Mechanics of Ocean Wave Interaction with Sediment Beds". Applied Ocean Research, 4, 99-106.